Hydrodynamic damping of solid and perforated heave plates oscillating at low KC number based on experimental data: a review

Mojtaba Ezoji[a], Naser Shabakhty[a*], Longbin Tao[b]

[a] *Department of Civil Engineering, University of Science and Technology of Iran, Iran* (* Corresponding Author)

[b] *Department of Naval Architecture, Ocean & Marine Engineering, University of Strathclyde, Glasgow, Scotland, United Kingdom*

Abstract

Heave plates exert a unique influence on the motions of marine structures floating in seas or oceans. Due to their low thickness and sharp edges, the hydrodynamic performance of these plates is influenced by such physical and oscillatory parameters as the Keulegan–Carpenter (KC) number, frequency, perforation ratio, cavity arrangement, cavity size, plate thickness, and proximity to free surface and sea floor. The present study tries to present an understanding of the hydrodynamic behavior of solid and perforated heave plates at low KC number by analyzing the flow regime and the related equations. Assessments have shown that at low a KC number, where the amplitude of oscillations is limited, the viscous damping derived from flow separation is proportionate to the area of the edges. Therefore, compared to solid plates, increasing the lengths of the edges by creating inner edges increases the viscous damping of these plates. Hence, in addition to solid plates, the performance of perforated plates has also been evaluated in this study. In this study, in addition to the other parameters, a new parameter – i.e., plate edges area-to-plate area ratio (Re/a) – has been used as basis to compare the results. Also, by investigating the experimental data of different researchers, a comprehensive study of the performance of heave plates will be provided. Finally, the parameters necessary for a better understanding of the hydrodynamic performance of these plates and the damping caused by the oscillations of a floating body in fluid will also be discussed.

Keywords: Solid Heave plate, Perforated heave plates, viscous damping

1. Introduction

In recent years, interest in developing advanced engineering systems based on fluid-structure interaction and vortex induced vibration has been increasing. One of the interesting topics of this field, which is emphasized in the marine industry in the form of oil platforms and renewable energy systems, is the unique effects of heave plates on the hydrodynamic damping of floating structures.

Many experimental and theoretical investigations have been carried out to understand the flow regime passing through thin rigid plates in fluids. The reason is that understanding this problem has important applications in the study of forces caused by submerged bodies oscillating and the hydrodynamic behavior (especially damping) of these plates in fluid. (Brown, 1964; Stephens et al., 1965; Woolam, 1978; Griffin and Ramberg, 1976; Dalzell, 1978; Singh, 1979; Graham, 1980; Bearman et al., 1985) Previous studies have highlighted the distinct advantages of these plate, so much so that by the end of the 90's, their use had become a necessity in many floating structures used to extract hydrocarbon materials (Fig. 1, right panel). The followings include some of these studies: Spars (Cavaleri and Mollo-Christensen, 1981; Glanville et al., 1991; Tao, et al., 1999; Tao and Cai, 2004; Zhou et al, 2013; Nallayarasu et al., 2014), Truss spar (Fischer and Gopalkrishnan,1998; Downie et al., 2000-A; Magee et al., 2000; Halkyard,1996; Kim et al., 1999; Wang, et al., 2001; Prislin et al., 1999), Tension Leg Platforms (Lake et al., 2000; Thiagarajan and Troesch, 1994) and Semi-submersibles (Roddier et al., 2009; Chakrabarti et al., 2007). These studies show that in extreme weather conditions,

particularly cases such as resonance motions, these plates can prevent damage in the sub-structural systems of floating structures (e.g., risers, excavation pipes, and bracing systems). Regarding this, Sudhakar and Nallayarasu (2011) showed that the maximum force acting on a Spar floating platform with a plate at the bottom is 30% lower than that of a classic Spar platform.

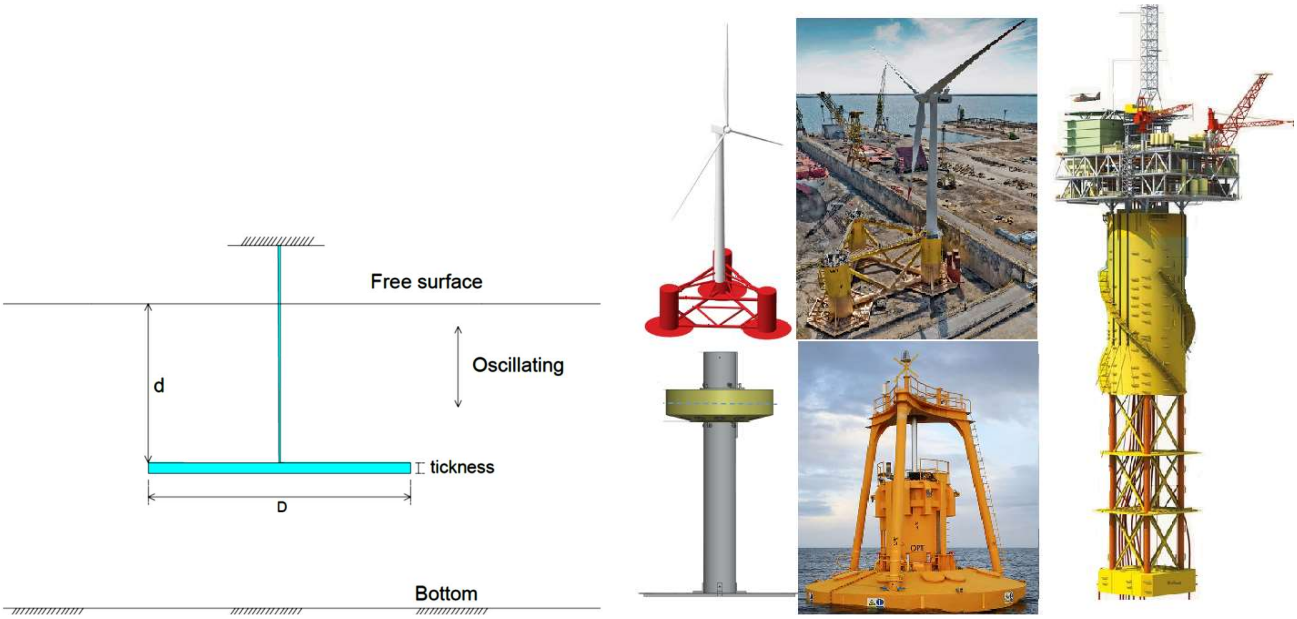

Fig. 1. Left panel: Geometrical properties; Right panel: Truss Spar (right side, Guardian, 2012), Wind Turbine (top-middle, Cermelli, C.A.,2014; top-left, Lefebvre and Collu, 2012) and Wave Turbine (bottom-left, Yu et al., 2018; bottom-middle, National Geographic, 2014)

Given the importance of climate change and the environmental policies of industrial countries, different energy-producing systems, i.e., floating wind turbines and wave energy converters, have been used from the start of the new century. In these systems, heave plates are one of the main subsystems. Some of these studies regarding this include: Wind Turbine (Kaufer et al., 2009; Jonkman and Buhl, 2007; Roddier et al., 2009; Subbulakshmi and Sundaravadivelu, 2016; Zhang and Ishihara, 2018; Karimirad and Moan, 2011); Wave converter (Coe et al., 2019; Penalba et al., 2018; Martin et al., 2019); Horizontal plate (McIver, 1985; Martin and Farina, 1997; Börner and Alam, 2015). In general, the aforementioned studies indicate that these plates increase the added mass, which keeps the resonant frequency of the floating body away from the frequency of first-order high-energy waves, without any change in the structural mass (Zhu and Lim, 2017). In addition to the added mass, the damping created by these plates is also very important, because the sharp edges of these plates can accelerate the vortex shedding process, which leads to the improvement of the system's viscous damping (Graham, 1976, 1980). Regarding this, Zhu and Lim (2017) showed that installing a heave plate on a cylinder increases the damping ratio of the cylinder by 200%. In general, the added mass and hydrodynamic damping of the heave plates can be important factors due to two reasons in controlling or decreasing the floating body's response in the acceptable range:

- It should be noted that due to the environmental conditions of seas, the hydrodynamic coefficients (damping and added mass) are not always beneficial. For example, by

evaluating the conditions of oil platforms, Li and Teng (2002) demonstrated that overly increasing the added mass causes the frequency of the oscillations to approach that of the waves. Therefore, increasing the added mass of a system does not always improve the stability performance of a floating body

- The marine structures go through a slow damping process. Due to the low oscillation amplitude of offshore structures, which stems different factors such as high draft and steady conditions of the sea in most days of the year (low KC), the viscous damping drastically decreases. Therefore, when the amplitude of the applied forces is small, it is possible for the system's response to be large due to the proximity of the waves' frequency to the to the resonant frequency. So, it is expected for the inertial force (added mass) to be dominant (Dowine et al., 2000 A) and not the viscous damping.

Therefore, to simultaneously tackle both of these challenges, i.e. logically increasing the added mass and creating additional damping, the present study, in addition to solid heave plates, it has been tried to describe the effects of perforations on the damping coefficient of heave plates. Many researchers have tried to perforate heave plates to increase edge length. The followings include some of these studies: (Taylor, 1956; Castro, 1971; Wood, 1964; Zdravkovich, 1981; Bernardinis, 1981; Chwang, 1983; Wu et al., 1998; Dowine et al., 2000 B; Molin, 2001; Evans and Peter, 2011; Malavasi et al., 2015).

Also, in addition to all of the aforementioned, at low KC number (KC≤1), the Morison equation does not yield accurate estimations for perforated, sharp-edged polyhedral bodies. In fact, there is no basis according to which the Morison equation can be used at low KC numbers, because no semi-steady drag is formed in the wake plates. Maull & Milliner (1978) recommended using the Blasius' equation to calculate the forces. However, calculation process is too complex. Therefore, because no accurate estimations have been provided for average force cycles in sharp-edged flat plates at low KC numbers, one of the main objectives of this study is accumulating and assessing the results of different investigations on flow regime at low KC numbers.

In flow regimes around sharp-edged flat plates, the forces are commonly expressed using appropriate values for the added mass and damping coefficients. These coefficients are functions of the Keulegan-Carpenter number and, to some extent, the frequency parameter (Keulegan and Carpenter, 1958),

$$KC = \frac{2\pi A_m}{D} \quad . \quad \beta = \frac{D^2 f}{\nu} \qquad (1)$$

in which β, A_m, D, f, and ν are the frequency parameter, the amplitude of oscillations, diameter of the plate, oscillation frequency, and kinematic viscosity, respectively.

At low KC (KC≤1), the amplitude of the oscillations is small ($KC = \frac{2\pi A_m}{D} < 1 \rightarrow \frac{A_m}{D} << 1$), the frequency of the oscillation is seen to have a little influence on the added mass coefficient for perforated and solid plate (An and Faltinsen,2013; Tao & Drayred (2008); Li et al., 2013). Therefore, the oscillation acceleration is very small ($\ddot{\eta} = A_{area}\omega^2 \sin(\omega t) \ll 1$, see Equation 2). In such cases, if perforated plated are used, due to the through of fluid flow by cavities, the added mass coefficient decreases with increasing perforation ratio at low KC number (Dowine et al., 2000 A, B; An and

Faltinsen,2013; Tao & Drayred (2008); Li et al., 2013). As a result, the effect of the first term of Equation 2 becomes smaller ($-A_{theoretica}\ \ddot{\eta}$). Therefore, it is expected that at low KC, the added mass coefficient of perforated and solid flat plates is almost independent of oscillation frequency. Also, it is noted that, the amplitude can also affect the damping as well as added mass when the plate is oscillating near free surface. Thus, most applications of heave plates to offshore structures have been trying to avoid such effect by placing the heave plates away from the free surface. The present paper focuses on the investigation specifically on hydrodynamic damping of heave plates oscillating at low KC number which is typical the heave plate applications to offshore structures. Under such low KC, the effect of amplitude on damping is relatively weak. However, as KC increases, such effect on both damping and added mass of heave plates oscillating near free surface can be significant. Also, in a 1998 decay test on isolated square plates, Prislin et al. (1998) showed that the damping coefficient in Reynolds number (Re>10^5) is dependent only on KC. To illustrate this dependence, some researchers have presented a new definition of KC (critical KC or perforation KC, Equation 12) (Molin and Nielsen, 2004; Molin, 2011; An and Faltinsen, 2013).

Hence, based on all of the aforementioned, the hydrodynamic damping of such plates is influenced by the following physical and oscillatory parameters:

- Oscillatory properties such as the Keulegan-Carpenter number and frequency
- Geometrical and physical properties of the plates including perforation ratio, perforation array, perforation size, thickness-to-edge ratio of the plates, proximity to free surface and sea floor.

Table 1: Investigation of geometric parameters in various studies

Subject	**Experimental**
The thickness	He et al., 2007; Tao and Dray, 2008; Tian et al., 2013; Li et al., 2013;
The size of the plates	Zhu and Lim, 2017; Zhang et al., 2018; Brown, et al., 2018; Abazari et al., 2019; Mahesh et al., 2021
The distances between multiple plates	Prislin et al., 1998; Abazari et al., 2019; Zhang and Ishihara, 2018; Mahesh et al., 2021; Mentzoni and Kristiansen, 2020
The perforation	Bernardini, 1981; Molin and Nielsen, 2004; Vu et al., 2004, Chua et al., 2005; Sandvik et al,.2006; Tao and Dray, 2008; Molin et al., 2008; Wadhwa et al., 2009; An and Faltinsen, 2013; Li et al., 2013; Malavasi et al., 2015; Tian et al., 2016; Brown, et al., 2018; Mentzoni and Kristiansen, 2019
The edge taper angles	Singh, 1979; Shen et al., 2012, Li et al., 2013; Mentzoni and Kristiansen, 2019
The distance of free surface	Molin et al., 2008; Wadhwa et al., 2009; An and Faltinsen, 2013; Li et al., 2013; Garrido-Mendoza et al., 2014; Lopez-Pavon and Souto-Iglesias, 2015; Thiagarajan an Menro, 2020;
Pattern of vortex shedding on plate	Singh, 1979; Bernardini, 1981; Thiagarajan and Troesch, 1994; Lake et al. 2000;
Current, Wave	Thiagarajan and Troesch, 1998; Mentzoni and Kristiansen, 2020; Thiagarajan an Moreno, 2020; Zhu and Lim, 2017;
Frequency of oscillation	Vu et al., 2004; Molin and Nielsen, 2004; Chua et al., 2005; Tao and Dray, 2008; Molin et al., 2008; Li et al., 2013; An and Faltinsen., 2013; Lopez-Pavon and Souto-Iglesias, 2015; Tian et al., 2016; Zhu and Lim, 2017;
Size of hole	Chua et al., 2005; Li et al., 2013; Tian et al., 2016; Mentzoni et al., 2019;
flexible plates	Zhang et al., 2020; Abazari et al., 2020

These parameters have caused the majority of studies on heave plates to be carried out on the geometrical properties of solid plates (Table 1). Abazari et al. (2020) evaluated the effects of non-solid of plates using compound solid-elastic plates (Fig. 5). The authors found that plate edges with lower stiffness (more elasticity) have a higher level of damping compared to solid plates. So, non-

solid plates can influence results. Therefore, in all tests, it has to be ensured that the plates are solid. To achieve this, Molin et al. (2008) used transverse stiffeners and Lopez-Pavon and Souto-Iglesias (2015) installed sensors on the plates. Also, to induce oscillations on the plate, Chua et al. (2005) used four bars on the four corners instead of a single central bar. This was done apparently to ensure that the same amount force was being applied to the four sides of the plate.

Based on what was discussed, this manuscript focuses on increasing our understanding of the hydrodynamic behavior of oscillating perforated and solid plates at low KC numbers by assessing the geometrical properties (Fig. 1, Left panel) and motion of these plates. By investigating the experimental results presented by other researchers, this study also attempts to provide a complete overview of the performance of heave plates and strives to evaluate the technical aspects of the Vortex Induced Vibration of floating bodies. The manuscript is composed of the following sections:

- Investigating analytical equations and oscillating experimental models
- The flow regime around the solid and perforated plates
- Describing the effects of free surface (this part includes two sections: plates in unbounded fluid and plates in the vicinity of free surface) and investigating the effects of frequency, perforation, thickness-to-diameter ratio of the plate, edges area-to-plate area ratio, distance ratio from the free surface
- The effects of scale on added mass and damping coefficients of heave plates

2. Forced oscillation tests

In many studies, a 3-D flow field, which is created from the interaction of a wave with a body, is approximated using a simple 2-D oscillating flow. This 2-D flow consists of two mechanical oscillators, one to simulate the oscillations of the structure, and the other to represent a nonlinear model of the fluid's behavior. These are known as the radiation-diffraction problem (Faltinsen, 1993). To simulate this challenge, two types of mechanisms have been used that can be divided into before and after the 90s. In the past, oscillation experiments were mostly carried out based on the diffraction model in U-tube water tanks (Singh, 1979; Sarpkaya, 1975) (Fig. 2, Right Panel). After the year 1990, however, with the advancement of experimental equipment, tests being were carried out based on the radiation model, i.e., the model in which the body moves relative to the fluid (Fig. 2, Left Panel). This type experiment can be performed in a tank or a small basin as well. Some of the geometrical properties and the employed equipment are given in Table 2. These equipment include:

- Load Cell: It was used to record the heave force on the plate system during the tests.
- LVDT (linear variable displacement transducer): It was used to verify the oscillation of the plate with the given displacement for the forced oscillating system.
- Vertical Planar Motion Mechanism (PMM) heave motion controlled by a planar motion mechanism.
- Potentiometer, piezoelectric, accelerometer: To measure the position, displacement and acceleration of disks.

Fig. 2. Right panel: U tube water tank (Singh, 1979), Left panel: Tank (side right, Tao and Dray, 2008), Basin (side left, Mendoza et al., 2014)

Table 2: Geometrical properties and employed equipment of some laboratories in many studies

	Name of the facility	**Country**	**Tank size in meters (Length x Width x Depth of water)**	**Loading Mechanism**
Singh, 1979	U tube water tank, Imperial College	United Kingdom	Diameter of tube: 0.61	
Lake et al, 2000, He et al., 2008	Marine Hydrodynamics Laboratory University of Michigan	USA	1.73x0.584x1.22	A vertically mounted shaker .
Vu et al., 2004	Laboratory at University of Western Australia	Australia	circular tank of 1m height and 1.65m in diameter.	The circular motion delivered by the motor was converted to linear motion using a ball screw and linear bearings.
Tao and Dray, 2008	Griffith School of Engineering, Griffith University.	Australia	4.940x2.120x 1.675	heave motion controlled by a planar motion mechanism (PMM)
Molin,2008	BGO-First facilities, in la Seyne sur mer (near Toulon).	France	40x16	
Wadhwa et al., 2009	Laboratory at University of Western Australia	Australia	1x1x (0.67~0.8)	Vertical Planar Motion Mechanism (PMM)
Tian et al, 2013	Shanghai Jiao Tong University	China	1x1x1.1	the crank is driven by a servo motor with a constant rotation speed.
Li et al., 2013	State Key Laboratory of Coastal and Offshore Engineering, Dalian University of Technology, China	China	60x4x2.5	servomotor
An and Faltinsen, 2013	the Marine Cybernetics Laboratory at the Norwegian University of Science and Technology,	Norway	40x10x1.4	vertical motion of the plate is excited by two vertically moving hydraulic actuators.,
Lopez and Souto-Iglesias (2015)	Technical University of Madrid (UPM), Madrid, Spain	Spain	100x3.8x2.2	electric actuator (FESTO DNCE 63-300-BS-10-PQ).
Abazari et al., 2019	Marine Ocean and Offshore Research (MOOR) wave tank, University of Maine	USA	8x1x (0.7~0.9)	A Parker ETH032 linear actuator driven by a 750 W Parker servo motor (Parker BE341F)
Mentzoni and Kristiansen, 2020		Norway	13.5x1x0.6	Actuater
Krish Thiagarajan & Javier Moreno, 2020	Marine Ocean and Offshore Research (MOOR) wave tank facility at the University of Maine	USA	8x1x (0.7~0.9)	a Parker ETH032 linear actuator driven by a 750 W Parker servo motor
Mahesh et al., 2021	Indian Institute of Technology Madras, Chennai, Tamil Nadu, India	India	90x4x2.5	Test decay: counter weight

3. Hydrodynamic equations based on the radiation experimental model

The total force caused by the oscillations of the radiation experimental model with the frequency ω includes components viscous damping (in-phase with oscillating velocity) and added mass (out-of-phase with velocity, or in-phase with acceleration). The damping and added mass terms are decomposed proportional to the square of the velocity, and the acceleration, respectively:

$$f_r = -A_{theoretica}\,\ddot{\eta} - B\dot{\eta} \qquad (2)$$

Wherein $\dot{\eta}$, $\ddot{\eta}$, and $A_{theoretica}$ are the oscillation velocity, the oscillation acceleration, and the added mass, which is equal to $\frac{1}{3}\rho d^3$ for isolated circular plates (Sarpkaya, 1981). Also, B is the strength (i.e., the damping) term, which determines the floating hydrodynamic specifications and is influenced by the square of the velocity difference between the oscillations of the fluid and the plate. In nature, each body has only one damping system. However, due to the high complexity of the governing equations, the system is subdivided into different components. So much so that the damping systems of plates oscillating in fluids are considered to be a combination of the structural damping (also known as fractional damping), radiation and viscous damping. The followings include of these strength terms:

- Given the small oscillation amplitude and independence from the Reynold's number, at a low KC number (which is the subject of this study), the effect of the frictional force with respect to the total drag force has to be a smaller than 2%~3% (Faltinsen, 1993).
- Radiation damping is completely under the influence of the free surface condition and is created by the interaction between the waves radiated by the oscillations of the model in the free surface. (Takaki and Lee, 2003) Therefore, in the oscillations of plates which are under the influence of free-surface conditions, radiation damping is dominant, which can create surface waves in the free surface.
- Viscous damping, which is influenced by the velocity difference between the oscillating plate and the surrounding fluid, creates a vortex shedding (Graham, 1980). This is affected by the edges of the plate. The experimental results reported by Sudhakar and Nallayarasu (2011) showed that for plates with high draft, radiation damping is a small fraction of viscous damping. Therefore, this type of damping is usually dominant at locations away from the free surface.

The effects of all of the aforementioned damping components are expressed in the form of a drag coefficient. This drag force is equal to:

$$F_{drag} = B\dot{\eta}(t) \quad \approx \quad F_{drag} = \frac{1}{2}\rho C_d A_{area}\,\dot{\eta}|\dot{\eta}| \qquad (3)$$

wherein C_d and A_{area} are the drag coefficient and the area of the solid plate, respectively. The drag coefficients are obtained via the Fourier averaging method (Sarpkaya, 1981) and using the eigenvalues of the velocity potential. Another method that can be used is the approach presented by An and Faltinsen (2013) which assumes the vortex to be symmetrical along the plates. By linearizing the nonlinear parameters, we would have:

$$C_d = -\frac{3}{4\rho A_{area}\eta^2\omega}\int_0^T F_r(t)\cos(\omega t)\,dt \qquad (4)$$

In most studies on damping, due to drag being dominant at low KC numbers and the simplification of the analyses, the damping term is linearized using Lorents' equivalent equation, i.e. $\cos(\omega t)|\cos(\omega t)| \approx \frac{8}{3\pi}\cos(\omega t)$. Therefore, drag and damping coefficients ($B\dot{\eta}(t)$) are linked via the Fourier analysis in the following form (Sarpkaya, 1981):

$$B = \frac{1}{3}\rho\upsilon C_d D\beta(KC) \qquad (5)$$

in which D, β, and υ are diameter of the plate, the frequency number, and the dynamic viscosity, respectively. Finally, the results are usually compared using the non-dimensional form of the damping coefficient (C_b), which is obtained by dividing the damping coefficient by $\omega A_{theorical}$:

$$C_b = \frac{4}{3}C_d(KC) \qquad (6)$$

C_b is under the complete influence of the KC number and the Cd coefficient. Also, since in the radiation model test, the oscillations are controlled by the operator, identifying the performance of the drag coefficient has been a priority for many researchers working on heave plates. Therefore, in the next section, we described this coefficient.

3.1. Drag coefficients of solid plate

Graham (1980) considered the average of the forces created by vortices proportional to the separation pattern and the Keulegan-Carpenter number, and presented the drag coefficient in the form:

$$C_d = A(KC)^{\mathrm{n}} \qquad (7)$$

n and A are non-dimensional coefficients.

3.1.1. The n coefficient

Graham (1980) considered this coefficient to be proportional with the separation angle of the vortices. The reason is that at low KCs number, the maximum displacement of the fluid particles in the unbounded fluid is a small compared to the dimensions of the plate. Therefore, it is impossible for the vortices to move away from the edges of the plate without significant oscillations (high KC), unless under the influence of the velocity field induced by the other vortices. Therefore, the separation angle is an important parameter in calculating vortex-induced forces, which are generally influenced by the shape of the edges of the plates (n):

$$\mathrm{n} = \frac{(3-2\lambda)}{(2\lambda-1)}, \qquad \lambda = 2 - \frac{\delta}{\pi} \qquad (8)$$

δ is the inner angle of the plate's edge at the separation point. For square flat plates, round edges, and other edges types, Graham (1980) proposed the values of 0, 90, and 0 to 90 for the parameter δ. Tao and Thiagarajan (2003-a) and Garrido-Mendoza et al. (2014) investigated the effects of shedding

angle. They specified that the sign of this angle is dependent not on the direction of movement, but on the condition in which movement starts. For the flat plates, Graham (1980) assumed n to be equal to -¾. For most KC number in the unidirectional regime, Lake et al. (2000) proposed the value of ¾ for n in the equation (7). But, Including the effect of the shape of the plate's edge in the damping coefficient proposed by Graham (1980) and Singh (1979) (Equation 7) is inconsistent with the results reported by Li et al. (2013) at low KC numbers for round edges smaller than 1 (λ=1). Li stated that the shape of the plate's edge does not affect the drag coefficients. This can be due to the different experimental setups, i.e. U tube water and forced oscillation tests. Based on the Li et al. (2013) study, in which the drag coefficient decreases as the KC number increases, Zhang (2018) made use of the equation $n = -\frac{1}{K_3}$, in which K_3 represents the shape of the plate and not the shape of the edge. For circular and octagonal of plates a value of 2.5 and for square plates a value of 3 is assumed for K_3. In any case, for square and flat-edged plates, the drag coefficient is a function of the expression $KC^{-\frac{1}{3}}$, which is similar to the results reported by Singh (1979).

3.1.2. The A coefficient

Graham assumed A as a function of the vortex force obtained from experiment. A is a non-zero empirical modification factor used to correct flow distribution in the outer edge of the disk or plate. Singh (1979) and Graham (1980) proposed, respectively, values of 8 (experimental result) and 11.8 (theoretical result) for A. By including the effect of the plate's thickness in the equation proposed by Thiagarajan and Troesch (1998) for the plate attached to a cylinder, Tao and Thiagarajan (2003b) defined the parameter as $A = \frac{t_{plate}}{d_{plate}}$. Also, using the data reported by Tao & Drayred (2008), Zhang (2018) defined the parameter as $A = 1.7\left(\frac{t_{plate}}{d_{palte}}\right)^{-\frac{1}{3.7}}$. Equations (9-a) and (9-b) have been proposed for the drag coefficients in the studies carried out by Tao and Thiagarajan (2003b) and Zhang (2018), respectively.

$$c_d = \left(\frac{t_{plate}}{d_{palte}}\right)(KC)^{\frac{3}{4}} \qquad (9-a)$$

$$C_d = 1.7\left(\frac{t_{plate}}{d_{palte}}\right)^{-\frac{1}{3.7}}(KC)^{-\frac{1}{K_3}} \qquad (9-b)$$

These equations are obtained by fitting the numerical results to the experimental data. It has to be noted that these equations lack generality and cannot be applied to other experimental results. But recommended, however, is that the equation proposed by Graham (Equation 7) can be used as a basis for equations predicting the drag coefficient of isolated plates which are away from boundary.

3.2. Drag coefficient for perforated plates

Perforated plates are quite suitable for the passive regulation of fluid flow and convectional heat transfer. For this reason, many researchers have tried to use perforated plates for the control and modification of flow using dimensional, analytical and semi-analytical models.

Based on the dimensional model, the effects of the perforations are expressed using the concept of dissipation factor. This dissipation factor is correlated with pressure drop and the corresponding average flow velocity (Euler dimensionless number).

$$\Delta p = f_f \frac{\rho U^2}{2} \rightarrow \quad f_f = 2\frac{\Delta p}{\rho U^2} \qquad (10)$$

in which U, f_f, ρ, p, and u are the apparent velocity of the fluid inside the porous medium, dissipation factor, fluid density, pressure, and average velocity of the fluid, respectively. $\frac{\Delta p}{\rho u^2}$ is the Euler number and is used as the pressure drop factor.

Based on the initial analytic model, the effects of perforations inside the medium are commonly evaluated using the Darcy (1856) equations. Assuming a very tiny size for the perforations (as a result, wake plate is laminar), Taylor (1956) and Chwang (1983 & 1998) used the Darcy model. In actual conditions, however, the pressure gradient in the perforations is nonlinear. Thus, Forchheimer (1901) defined the non-dimensional pressure drop as follows:

$$f_d = \frac{D_h}{L}\frac{\Delta p}{\rho u^2} \qquad (11)$$

wherein L and D_h are, respectively, the thickness of the plate (or the thickness of the porous medium) and the hydrodynamic diameter of the empty spaces and the perforations. Furthermore, Benjamin et al., (2012) introduced the non-dimensional form of the Darcy-Forchheimer (D-F) model. Also, Tanner et al., (2019) showed that in plates with a single large perforation at very small Reynolds numbers, there are parts of plate in which pressure drop is independent from the Reynolds number. In similar studies, e.g., Bayazit (2014) and Malavasi et al. (2012), similar results were obtained. In general, the result of conclusion being that at Reynold's numbers higher than the threshold, pressure drop is dependent on other parameters such as perforation and the $\frac{t}{D_h}$ ratio.

Also, using a semi-analytic model which is based on the assumptions of the potential theory (e.g., non-rotational), a series of equations were proposed by Molin (2001). The most important point of the proposed method is that the hydrodynamic coefficients for added mass and the damping are functions of the amplitude of motion. In this method, similar to the Darcy model, it is assumed that the plate's thickness is very small and that the plate contains infinite perforations. In general, for perforated plates, the effects of the plate's perforation have to be taken into account in the above-mentioned model. These effects include:

a. Modifying the area of the plate (using perforation ratio in the drag force equation), for plates with non-continuous perforations and grid plates this value is, respectively, equal to $z = \frac{aperture\ area}{solid\ area}$ and $z = 1 - \frac{nd}{D}$, in which n is the number of bars, d is the diameter of each bar, and D is the diameter of the plate.
b. Taking into account the average velocity along the length of the plate ($\overline{U} = \frac{U}{z}$), pressure drop distribution in perforation plates is similar to an inverted u shape. Pressure distribution

on perforated plates is similar to that in solid plates (Faltinsen, 1993-analytical method for solid plates & Mentzoni et al., 2020-experimental method for grid plate).

c. Introducing the nonlinear pressure drop parameter μ into the drag equation to consider the effects of the perforations, using this parameter, Molin (2001, 2004) tried to include the effects of pressure drop in the equations in the form of a strength coefficient (κ), and used the inverse pressure drop coefficient (1/μ) in place of the Morrison drag coefficient ($\kappa \propto 1/\mu$). Various references usually consider the ratio $\frac{\Delta P}{\rho u^2}$ (Euler's non-dimensional number in equations 10 and 11) as the strength coefficient (κ). This coefficient, which contains the intrinsic pressure drop characteristics caused by friction, drag, and normal stresses, is completely dependent on the perforation ratio, defined by Molin, (2011) as $C_d \propto \frac{1}{\mu}\frac{(1-z)}{z^2}$. The parameter μ is usually between 0.5 and 1.

By considering what was discussed above, the damping of plates is influenced by the Keulegan-Carpenter functions (amplitude oscillations and dimension of the plate) and the perforation ratio. Therefore, the local Keulegan-Carpenter number or perforation Keulegan-Carpenter number was defined by Molin (2001) and Molin & Nielsen (2004).

$$\widetilde{kc}(por) = \frac{\eta}{D}\frac{(1-z)}{2\mu z^2} \qquad (12)$$

D and η are the diameter and amplitude of motion of the plate, respectively. It has to be mentioned that Molin formulated the above-mentioned equations with the assumption that the plates are thin and that there are infinitely many very small pores (local inertial effects are insignificant). Then, by defining the perforation Keulegan-Carpenter number, the effects of pore-induced damping (PID) were taken into account. This way, the pressure differential is only related to the average of the square of the translational velocity, meaning that the flow/plate velocity is not taken into account. Therefore, the equations only consider the effect PID. However, it is important to also account for the effects of the plate's edges and their effect on damping. For this reason, Sandvik et al. (2006) introduced the plate relative velocity – which is equal to the difference between the average plate velocity and the average velocity of the fluid passing through the pores ($\overline{\dot{\eta}_r} = \overline{(\dot{\eta} - \dot{\eta}_p)}$) – into the drag force equation. This was done to account for the effect of flow separation at the end of the plate. Therefore, we have:

$$\Delta P = \frac{1}{2}\rho C_d A_{area}(1-z)\overline{\dot{\eta}_r}\,|\overline{\dot{\eta}_r}| \qquad (13)$$

In the pore configuration section, we will discuss in what parts, pores, and edges separation has the highest influence.

4. Flow physics

Our understanding of the hydrodynamics of thin plates oscillating at low KC numbers is very limited. This is because unlike what is seen in cylinders (Sarpkaya, 1981), the drag force is more complicated than the inertial force at low KC numbers (Graham, 1980). One of the ways of having a better understanding of the flow regime around these plates is to use the flow visualization

method for evaluating the physics of the flow. This way, the effects of different parameters will be suitably identified, and they can be even introduced into the equations. Multiple studies have been carried out on this subject. Using this method, Singh (1979) defined different flow regimes on both sides of a solid vertical plate at different KC numbers, while the system was under the influence of in-line forces (Fig. 3):

- Symmetric, KC<3: In this regime, considering that the flow amplitude is small, flow does not quite develop around the plate. In this regime, shear layers develop symmetrically and the vortices are weak on both sides of the edge. Therefore, there is no interface between the shear layers.
- Anti-symmetric, 3<KC<7: In this regime, as the KC number increases, the shear layers separated from the edges on both sides of the plate start to make contact (share an interface), leading to the rise of a vortex on one of the sides, which is faster and larger. When the flow is reversed, some of the flows move under the plate, appearing as a weak jet. Then, as the flow develops, a new vortex starts to take form in the lower edge.
- Cycle, 7<KC<25: In this regime, the flow pattern is quite stable and cyclic which would persist for hours after adjustment. It appears that the prerequisite for the development of this regime is the complete development or shedding of a vortex in each cycle. In this regime, various stable vortices occur in one side of the edge in each semi-cycle, which often occupy the entire width of the plate. In the following, while this strong vortex is shed, it draws the weaker vortex on the other edge towards it and then be shed as a jet-like manner.

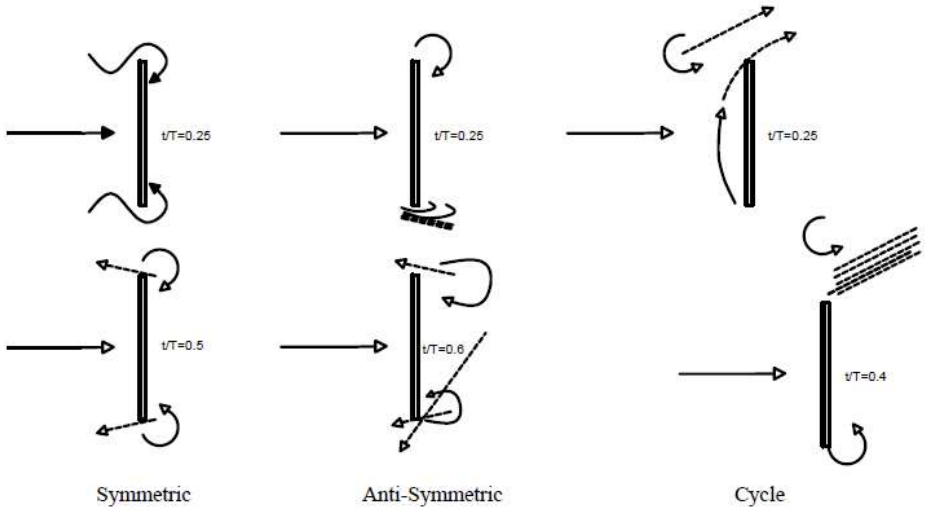

Fig. 3. Flow physics on both sides of a solid vertical plate, in-line flow (Singh,1979)

The Singh's flow pattern related to both sides of the vertical plate is completely under the influence of the KC number and the diameter of the plate. However, flow pattern related to both sides of the horizontal plate completely different. In a numerical investigation, Graham (1980) and Bernardinis et al. (1981) defined the flow regime around the edges of thin plates as independent, interface, and Uni-directional, emphasizing the importance of the thickness of the plates and how it affects the flow pattern around these plates. Also, with the help of flow visualization, Thiagarajan and Troesch (1994) asserted that at large KC numbers, the flow pattern around the edges of the plate

is completely anti-symmetric. Other studies have also been carried out on this subject by Sireta et al. (2008), Rusch et al., 2020 and Mentzoni et al. (2020). By defining a critical KC number and with the help of the drag variation curve, Tao and Thiagarajan (2003-b) categorized the flow regime amplitude of horizontal oscillating plates into three regimes at low KC numbers (Fig. 4).

- Independent: In this regime, at high thickness to diameter ratios, two negative vortices, which are created on top and beneath the plate due to the plate's downward movement, do not come in contact and behave independently from one another.
- Interface: This regime usually appears at an earlier stage in thinner plates, because the shear layers on the top and bottom come in contact. In this regime, when the plate moves downward, the vortices on the lower edge join the stronger upper vortices (these two vortices have the same sign), resulting in the creation of an even stronger vortex pair on the upper edge. It has to be mentioned, however, that no interaction takes place between the upper and lower vortices in a full cycle.
- Uni-directional: Similar to the previous regime, this regime appears at thickness to smaller diameter ratio of the plate. In this regime, powerful negative vortices are created when the plate moves downwards. These vortices collide with the strong positive vortices created in the previous semi-cycle when the plate was moving upwards. In the following, when the direction of motion reverses, an interaction between these two negative and positive vortices takes place, resulting in the coupling of the two vortices. Finally, because the negative vortex is a stronger, the two vortices (the negative and positive vortices) are shed as jet at an angle from the axial direction.

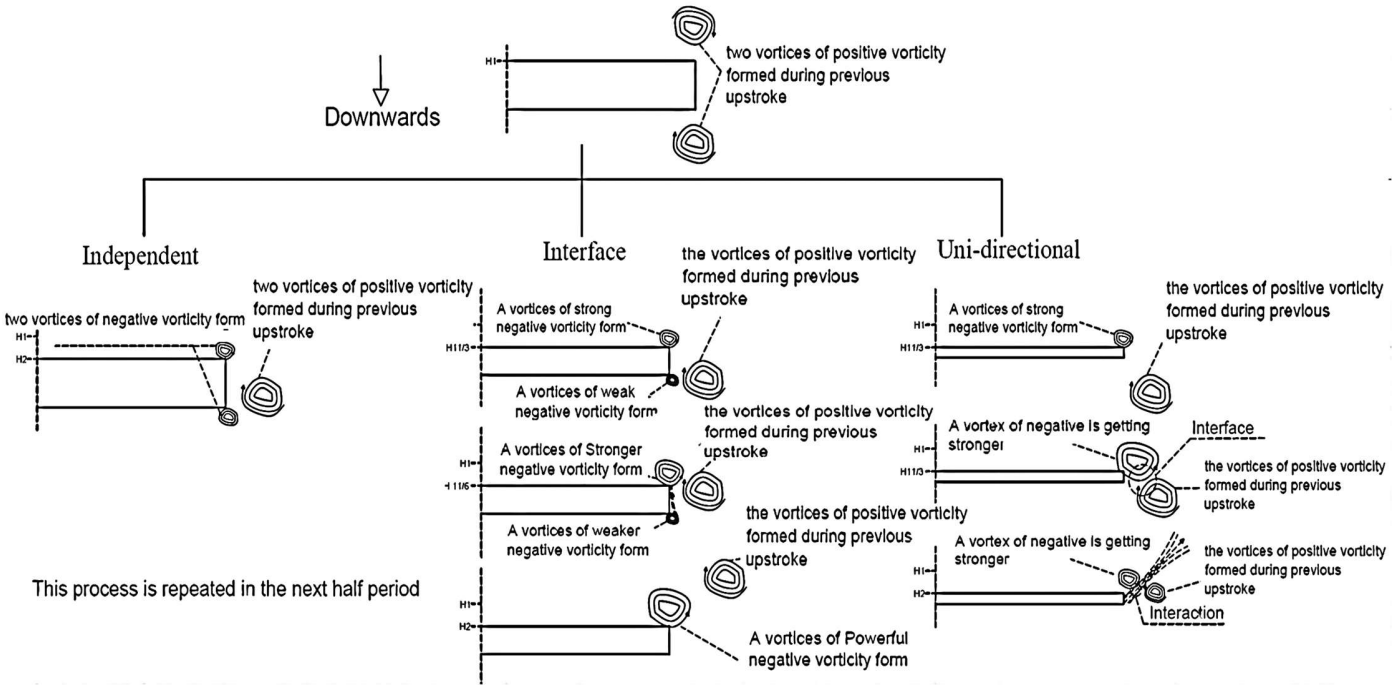

Fig. 4. Flow regime of horizontal oscillating plates (different thicknesses) at low KC

Tao and Thiagarajan (2003a) showed that this angle is not dependent on the fluid's free surface and the plate's thickness-to-diameter ratio. It is, however, under the complete influence of the KC number, so much so that when the KC number increases, the angle also experiences an increase. It should be mentioned that at low KC numbers, the slope of this increase is more noticeable. In the studies on flow regimes of vertical and horizontal plates, in cyclic and unidirectional regimes, this angle is slightly different. In the case of vertical plates, the shedding angle only occurs at high KC numbers and is diagonal with respect to the direction of the flow. However, in horizontal plates, the angle tends toward axial and the diagonal directions at low and high KC numbers, respectively (Graham, 1980).

Finally, Studying the physics of the flow on both edges of vertical and horizontal plates shows the influence of a dimensionless geometrical parameter – i.e., thickness to diameter ratio of the plate. For very small thickness to diameter ratios (e.g., smaller than 0.01), this ratio causes the unidirectional flow to happen at a much smaller KC. Therefore, considering the thickness-to-diameter ratio, it is possible for one regime to occupy at larger range of KC numbers. For this reason, when the interface regime is been changed into a unidirectional regime, we will witness a translational zone at low KC numbers (He et al., 2008). It is more probable for the damping peak to happen in this translational zone. This, however, requires more investigation. Overall, studying the physics of the flow and equations around heave plates reveals that the hydrodynamic performance of the plates is influenced by boundary conditions, physical properties, and oscillation parameters. In the next section, investigated these parameters.

5. Effect of boundary conditions on the damping coefficient of heave plates

Due to the influence of free-surface boundary conditions on the damping coefficient, this section will be presented in two subsections:

- Plates in unbounded fluid
- Plates close to free surface

In this section, the influence of the conditions of the fluid's free surface on parameters such as frequency and perforation will be investigated. Due to the different uncertainties associated with the carrying out of a test, the experimental results reported by different researchers will be compared. The final trend of these results will then be taken as a basis for this study. For this, influential parameters such as thickness-to-diameter ratio of the plate, edges area-to-plate area ratio, and the ratio of distance from the free surface to the diameter of the plate (obtained from the studying the physics of the flow) will be used.

5.1. The effects of unbounded fluid condition on the damping coefficient of plates

5.1.1. Solid plates in unbounded fluid

As shown in the flow physics and equations sections, one of the parameters affecting the hydrodynamic behavior of plates in unbounded fluid's is the thickness of the plate. Through wind tunnel experiments on vertical plates, Bayazit et al. (2014) showed that in turbulent flow, thinner plates cause a larger pressure drop compared to thicker plates. Regarding this, Lake et al. (2000)

stated that at low KC numbers, plate thickness (thickness-to-dimension ratio, t/d ≈ 0.0416) influences the coupling of newly-formed vortex rings with the vortices created in the previous cycle. Therefore, to compare different studies, the experimental results have been presented using a non-dimensional t/d ratio parameter (Fig. 5, right side). In this figure, the results of Lake et al. (2000) (brown plus) and He et al., (2008) (green line) show similar damping coefficients for t/d ratio of about 0.04 (these two studies, as indicated in Table 2, have been performed in the same site). Also, He et al., (2008) (red line) and Tian et al. (2016) (blue circles) show similar damping coefficients for t/d ratio of about 0.03 at KC>0.4. As seen in the left side of Fig. 5, Li et al. (2013) (black squares) and Vu et al. (2004) (purple circles) have reported similar damping coefficients for t/d ratio of about 0.01. Furthermore, the studies of Chua et al. (2005) (blue circles), Tian et al. (2016) (green triangles), and Tao and Drayred (2008) (red squares) also report almost identical results for the t/d ratio of 0.02.

In general, by comparing the results of these studies (shown in Fig. 5 & 6-left side), it appears that by increasing the t/d ratio, the damping coefficient decrease at similar KC numbers. The same results can also be seen in the studies of other researchers (He et al., 2008; Chua et al., 2005, Li et al., 2013-left side). but, comparing the data shown in Fig. 5 (left side) shows that although the studies of Chua et al. (2005) (blue circles), Tian et al. (2016) (green triangles), and Tao and Drayred (2008) (red squares) have had a larger t/d ratio than the studies of Li et al. (2013) (black squares) and Vu et al. (2004) (purple circles), they have higher damping coefficients. This means that the t/d ratio might not be a reliable basis of comparison for the experimental results reported by different researchers. Therefore, another parameter capable of accounting for all of these properties should be used.

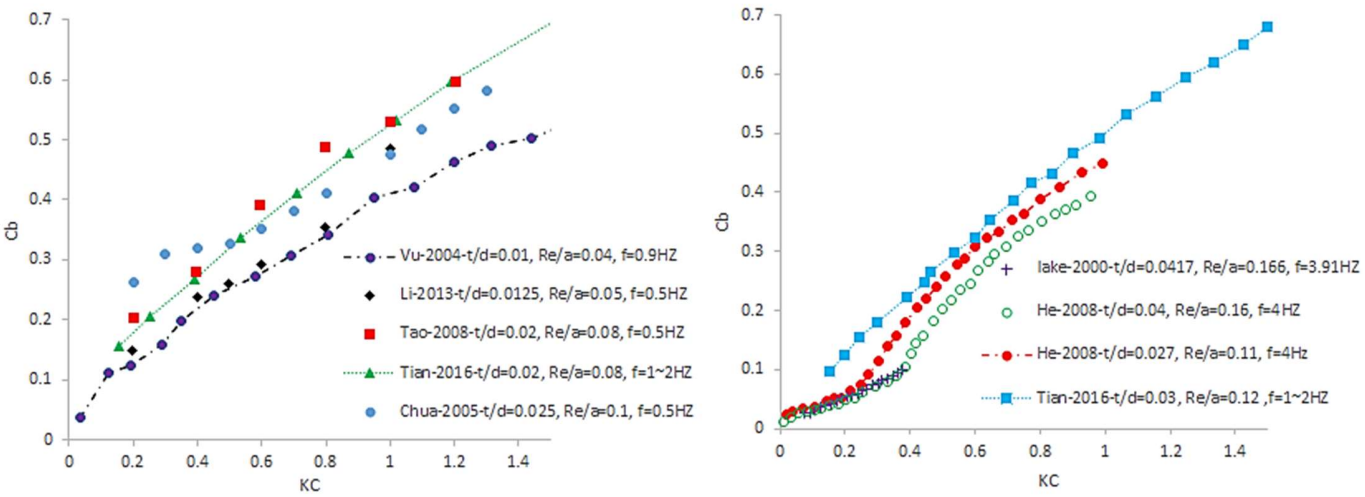

Fig. 5. Comparison of experimental results of solid plates in unbounded fluid

The flow physics study in the previous section showed that in addition to the thickness of the plate, the plate's edge is also an influencing factor because of the inherent continuity and cohesion between the vortices created around the edges. furthermore, the area of the plate is important due to its influence on inertia (McNown et al., 1959). Therefore, in this study, in addition to the other

parameters, a new parameter – i.e., plate edges area-to-plate area ratio (Re/a) – has been used as basis to compare the results.

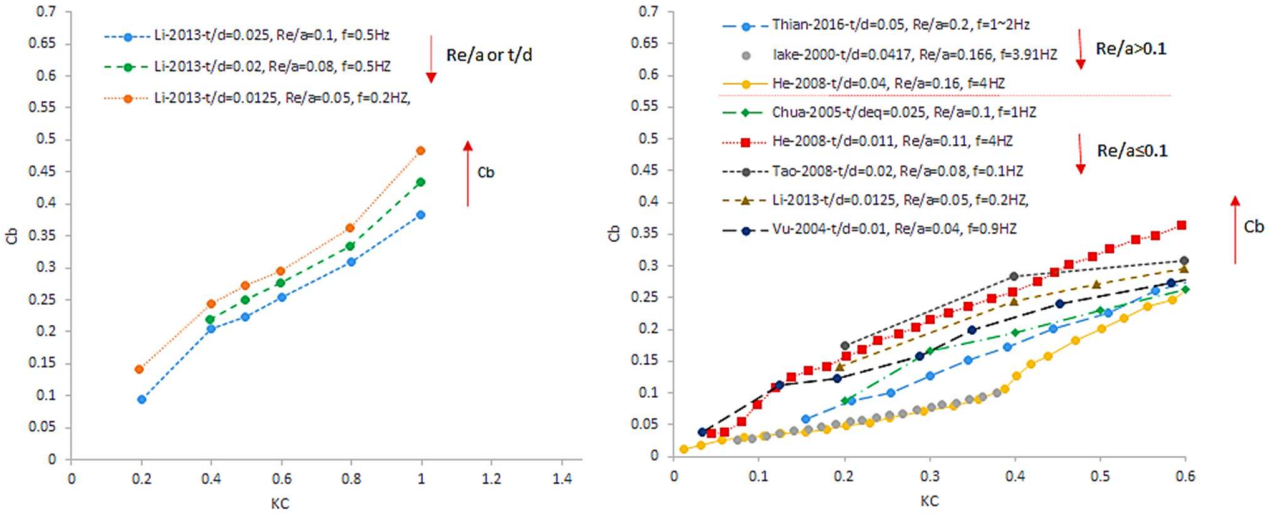

Fig. 6. Comparison of experimental results of solid plates in unbounded fluid (Left side-Li et al., 2013; right side-other studies)

The Re/a ratio is a reliable parameter at low KC numbers. The reason is that the effects of added mass on damping coefficient – which are in the equations describing the Cd coefficient – are taken into account. Also, the results of the square and rectangular plates can be compared. In conjunction with the t/d ratio parameter, this newly-defined parameter is used to compared results of different studies on unbounded fluids (see Fig. 6,). As seen in Fig. 6 -right side, the parameter Re/a provides a better comparison of the results of different studies investigating models with varying geometric properties (Table 3). By decreasing the ratio to Re/a>0.1 (Fig. 6, right side), we witness an increase in the damping coefficient in all of the studies. further decreasing the value of the ratio (Re/a<0.1) leads to a decrease in almost all of the damping coefficients. It has to be mentioned that at the values smaller than 0.1 (Re/a<0.1), scatter and irregularity can be seen in some of the oscillation ranges. This phenomenon might be due to another parameter (e.g., frequency). Therefore, the effects of frequency will be discussed in the followings.

5.1.2. Effect of oscillation frequencies on solid plates

It is expected that frequency dependence of the damping coefficient of the solid plates is not pronounced at low KC oscillation in unbounded fluid domain. Because, the non-dimensional damping coefficient equation (Equation 6) shows that the frequency term has been removed from the equations in order to make them non-dimensional. But, through experimental investigations Vu et al. (2004) and Chua et al. (2005) highlighted the sensitivity of the damping coefficient to changes in frequency at low KC numbers. But, Li et al. (2013) showed that for KC>0.2, the drag coefficient of plates in unbounded fluids is not influenced by the frequency parameter (Fig.7, right side). This has been corroborated by the results reported by Tian et al. (2013).

Fig. 7 presents the results of the studies performed by Chua et al. (2005), Li et al. (2013) and Vu et al. (2004) for isolated rectangular plates in unbounded fluids at frequencies lower than 1 Hz. In all of these studies, the t/d ratios and the e/d ratios of the plate are almost identical. According to this figure, frequency changes do not exert a meaningful influence on the damping coefficient-KC number curve.

In general, there is a contradiction between the results of different researchers regarding the dependence of the damping coefficient on frequency. For example, unlike the studies mentioned above, the results reported by Abazari et al. (2019) shows that frequency changes can significantly alter the overall trend of the damping coefficient-KC number curve. Tao & Drayred (2008) have emphasized the low sensitivity of the damping coefficient to frequency. However, Tian et al. (2016) stipulated that frequency exerts either no influence at all or significantly changes the damping coefficient-KC number curve. The reasoning of the authors for the latter is that the hydrodynamic force exerted on the plates is proportional to the square of the frequency variable. Therefore, the changes of the damping coefficient with respect to frequency should also be of the second order (similar to the results of Abazari et al. (2019)). The results reported by Tian et al. (2016) invalidated the claims made by Tao & Drayred (2008) regarding the low dependence of damping coefficient on frequency.

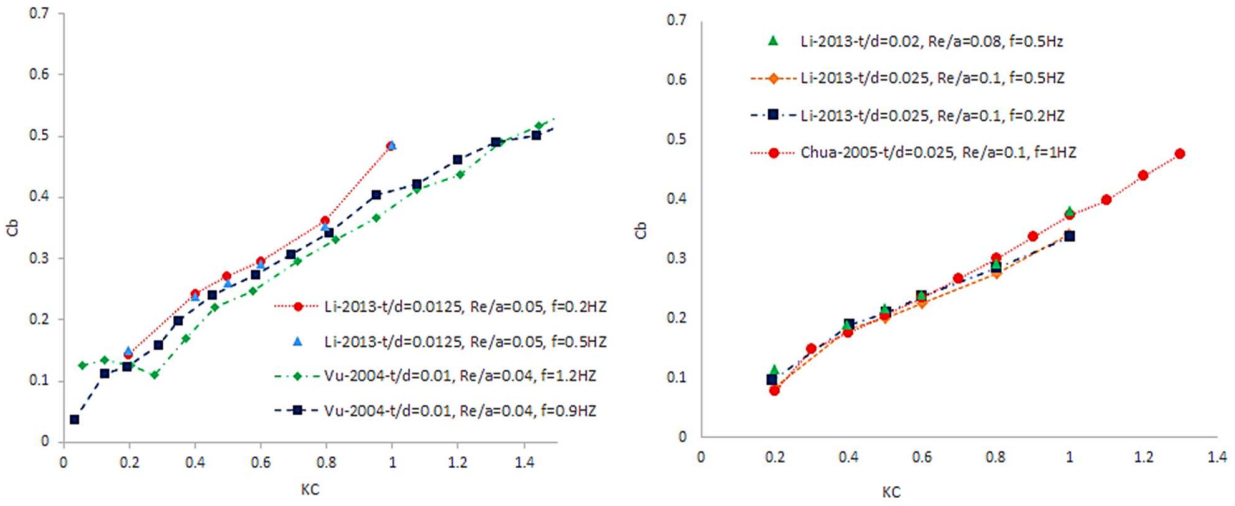

Fig. 7. Comparison of solid rectangular plates at different frequencies

Assessing the equation of the non-dimensional damping coefficient (Equation 6) shows that there is no direct correlation between the damping coefficient and frequency of oscillations. However, the frequency may affect the damping coefficient slightly which can be demonstrated by solving the integral part of the drag coefficient equation (Equation 4). To ensure a reliable review of the effects of frequency change on the damping coefficient, the experimental results of Tao, Chua, and Tian, which have similar t/d and Re/a ratios, have been compared (Fig. 8-left side). According to this figure, the influence of frequency on the damping coefficient is low, meaning that one should not expect for the effects of frequency on the damping coefficient to be of the second order and to fundamentally shift the overall trend of the damping coefficient-KC number

curve. It has to be mentioned that this conclusion only holds true if the heave plates do not have a motional phase difference with the waves (similar to spars). Otherwise, it appears that change in the oscillation frequencies of these plates brings about changes which go far beyond scatter in the damping coefficient curve (similar to wave energy converters).

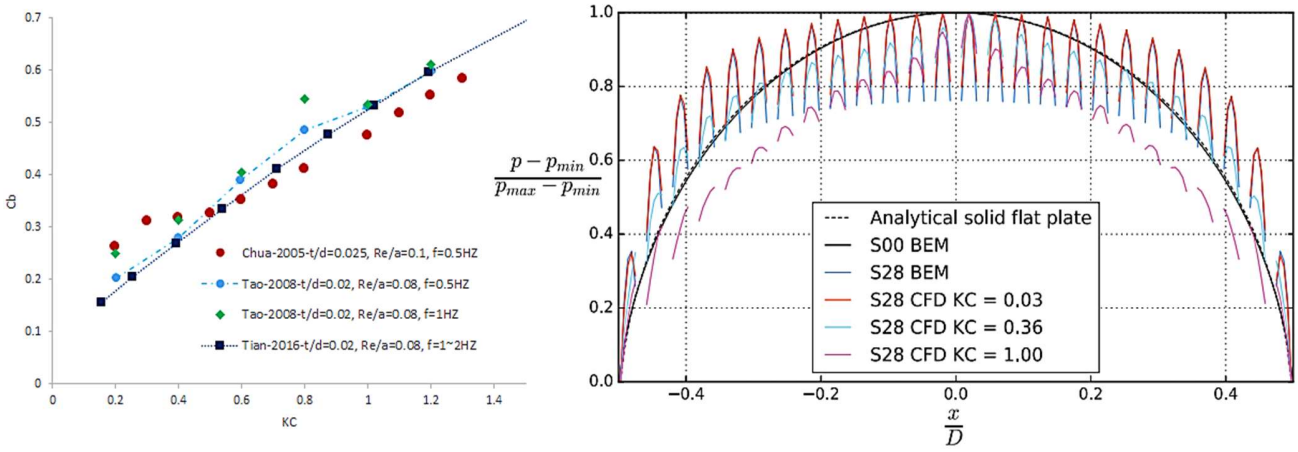

Fig. 8. Comparison of solid rectangular plates at different frequencies with Re/a and t/d similar (left side), overall pressure drop distribution in perforation plates (Mentzoni and Kristiansen, (2020)-right side)

In any case, the above-mentioned contradictions might be due to the conditions of the laboratories. Because of;

A) To simulate the actual conditions in experiments: in most tests involving the radiation model, researchers try to keep oscillations within the resonant of the frequency range. As a result, the drag coefficient is under the influence of the natural and resonant frequencies of the system. For plates connected to cylinders (which have the same surface as the free surface), these resonant frequencies are easily calculated. For example, in an experiment on a plate connected to a cylinder, Thiagarajan and Troesch (1998) used a full-scale model's (including the cylinder and the plate) natural frequency of about 0.41 Hz to apply the vertical oscillating force. Also, Tao et al. (2007) used the very low frequency of 0.035 Hz (which falls into the natural frequency range of the scaled cylinder-plate model under study) to carry out numerical simulations. But the resonant frequency cannot be clearly identified in tests involving isolated plates: Fist, the resonant frequency of these plates happens at small values. The reason is the low thickness of most heave plates, causing them to behave similar to a slender element (e.g., mooring lines). This is the reason why the resonant frequency of these plates takes place at low frequencies. Second, the isolated plates are jointed to a planar motion mechanism only using slim rebars. So, they have a low water plan at the free surface. Therefore, finding the natural frequency of isolated plates is difficult. Third, since the plate is oscillating in a stationary water, we are only dealing with the experimental radiation model. This issue causes the conditions of the experiment on isolated plates not to be ideal. The reason is that instead of the frequency of the waves, the frequency of forced oscillations must be used as the reference parameter. Fourth, in lieu of the mass of the entire body (the cylinder and the plate), the added mass of the plate should be used make the damping coefficients of isolated plates non-dimensional. However, instead of the KC number, some researchers (e.g., Lopez-Pavon and Souto-

Iglesias (2015)) have tried to explain these effects using the ratio of angular velocity of oscillations to natural oscillations (ω/ω_r).

B) Laboratory equipment: dimensions of the tanks used in different experimental setups (given in Table 2) to influence the boundary conditions.

C) Different test conditions: For example, Chua et al. (2005) used 4 rods to apply force on the four corners of the plate, whereas Li et al. (2013) employed a single rod in the middle of the plate.

5.1.3. Effect of perforation plates on the damping coefficient

The mechanisms of creating resisting (damping) forces by oscillating solid heave plates stems from the pressure difference in the field around the plate. This leads to a difference in velocity in the movement field of the fluid around the plate, causing flow separation and vortex shedding in the plate's outer edges. Therefore, the local flow around the plate's outer edges and a small component of the surface shear are the main reasons of damping at low KCs (Lake et al., 2000). These results reveal that one of the solutions to increased damping is to increase the area of the edges. This can be achieved by creating inner edges (via perforations and holes) throughout the area of the heave plate.

Solid and perforation plates create these resisting forces through different ways. In solid plates, damping is created from flow separation and the formation of a vortex shedding only from the outer edges. In perforation plates, by contrast, in addition to the outer edges, the inner edges (perforations) are also involved in the damping process (Wang et al., 2002). Regarding this, Mentzoni and Kristiansen (2020) showed that the effect of flow separation in the outer edges is more important than in the inner edges. This can be due to two reasons: the first reason is that similar to solid plates (Faltinen, 1993), the overall pressure drop distribution in perforation plates is in the shape of an inverted U (Fig. 8-right side). This means that pressure drop in the outer edges is higher than it is in the inner edges. The reason is that in the outer edges, there is an evident discrepancy between the velocities of the particles of the fluid in the edge and the outer area surrounding the edges. In the inner edges, however, this velocity difference is a smaller on the top and bottom of the plate and in the locations of the perforations. Therefore, it is expected that stronger vortices to be created in the outer edges. The second reason is the non-distribution of reinforcing pressure in the perforations by increasing the KC number. In this case, pressure distribution in the edges is normal. Because by increasing the KC number, the pressure distribution curve becomes smoother, to the point that even the level of pressure drop in the locations of the perforations is lower compared to the same locations in solid plates. In this condition, the flow has a more uniform pressure distribution, similar to the wake of a cylinder (Mentzoni and Kristiansen, 2020). However, at low KC numbers, the level of pressure drop in perforated plates is higher than solid plates in the locations of the perforations, which needs to be studied further.

Fig. 9 presents the results of the study carried out by Li et al. (2013), An and Faltinsen (2013), Mentzoni and Kristiansen (2020), Sandvik et al. (2006), and Tian et al. (2016) for rectangular plates with similar perforation ratio, but different thickness-to-diameter ratios and frequencies. All of these studies reported similar results. This can also be seen in the results of the studies carried out by Tao and Dray (2008) and Vu et al. (2004) in which identical porosities and different thickness-to-

diameter ratios have been used (Fig. 10, right side). These results, therefore, highlight the importance of using a more reliable parameter (i.e., perforation) over other parameters.

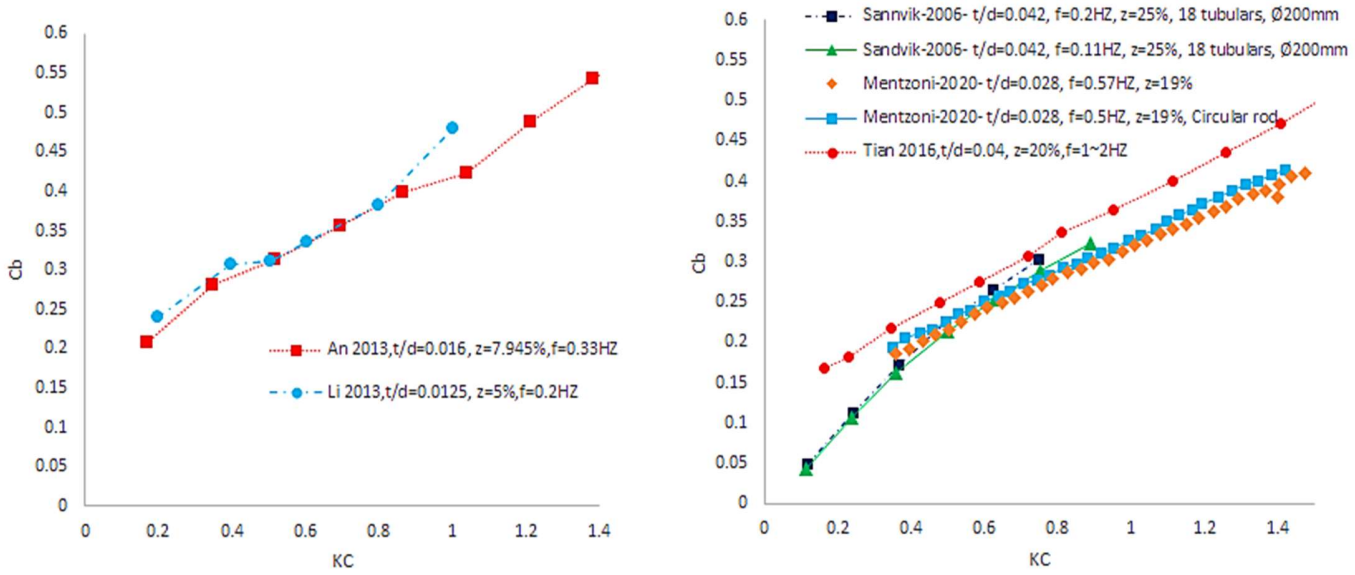

Fig. 9. Comparison of perforation plates with similar perforation ratio

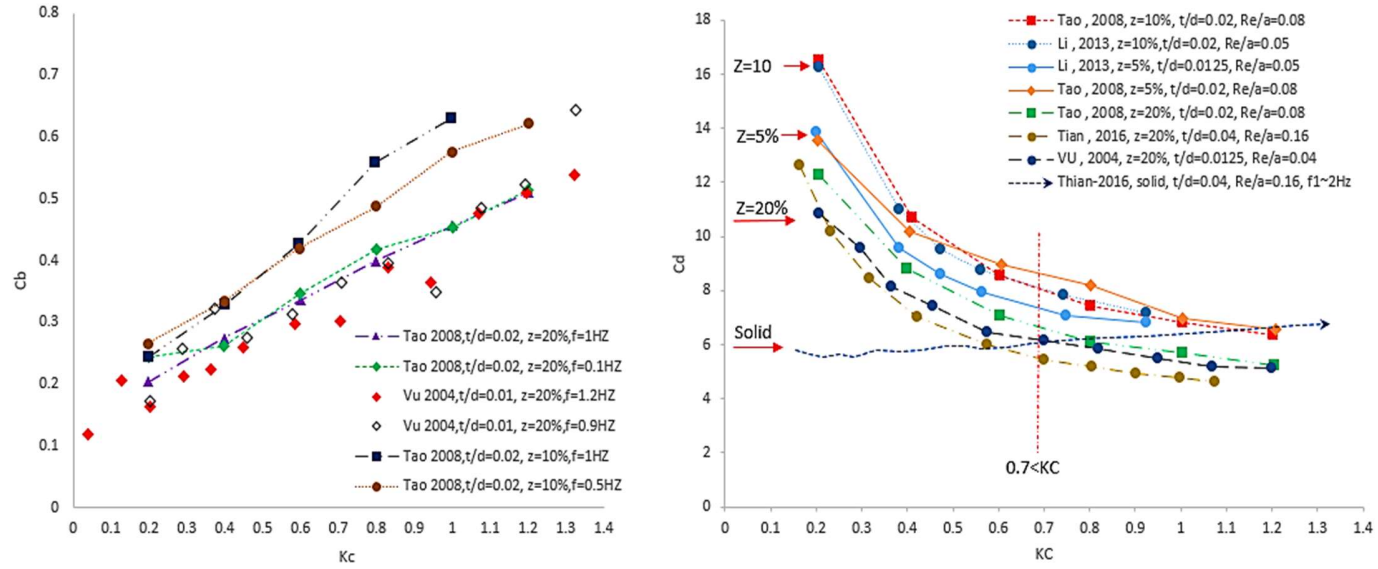

Fig. 10. Comparison of the perforation plates with different porosities and similar t/d ratios (cb-left side, cd-right side)

The studies (Fig. 10, left side) show that as perforation increases, the damping coefficient also experiences an increase. Li et al. (2013) demonstrated that by increasing perforation (from 0.0 to 10%) and the KC number (from 0.2 to 0.8) always results in an increase in the drag coefficient. Upon reaching a KC number of 1, the drag coefficient becomes equal to that of solid plates. Also, Fig. 10 by increasing perforation (from 10% to 20%), the damping coefficient experiences a

decrease. Regarding this, Tian et al. (2016) showed that the highest value for the drag coefficient occurs at a KC number and perforation of 0.6 and 10%, respectively (Fig. 10, right side).

Tao and Dray (2008) carried out experimental forced oscillation investigations at different frequencies with porosities ranging from 5%, 10% and 20% (Fig. 10, left side). The authors found that the hydrodynamic damping of an oscillating perforation plate is more sensitive to the amplitude of motion and less sensitive to the oscillation frequency, especially at KC ranging from 0.8 to 1. They also showed that by increasing the perforation of plates that are away from the free surface, the influence of frequency becomes more pronounced. The results showed that at low KC numbers, frequency does not exert a significant influence on the damping coefficient of plates with low perforation. However, this is still expected to cause some scatter in the damping coefficient. This is similar to results obtained for solid plates.

In general, there are two important points in the results of the mentioned studies. The first point is that at low KC numbers, as the perforation increases to about 15%, the damping coefficient increases compared to solid plates. Then, as the perforation increases further, the damping coefficient experiences a decrease. This is due to the disturbance in the flow of fluid in the wake of the plate, which prevents the creation of a vortex. The second point is that as the KC number increases (until KC>0.1), the influence of perforation increase on the drag coefficient becomes considerably weak, so much so that further increase in the perforation of the plate causes the drag coefficient to fall below that of solid plates (Fig. 10, right side). This conforms to the results of the analytical study carried out by Molin et al. (2001). Molin et al. (2001) demonstrated that at KC>1, the damping of perforation plates cannot be higher than that of solid plates.

5.1.4. The effects of perforation shape, dimension, and holes array of perforation plates on the damping coefficient

The studies mentioned in the previous section showed that perforation is an important parameter. However, since pressure drop in the plates is U-shaped, the perforations become more influential if they are closer to the edge of the plate. Because decrease in pressure is higher at the edges. Therefore, it would be logical to expect that the array, number, and size of the perforations on heave plates to influence the damping coefficient.

In 2019, through an experiment performed in a horizontal channel on vertical plates with constant perforation and two types of perforations (a large hole in the middle and smaller holes over the entire area of the plate), Tanner at el. (2019) showed that difference in pressure drop between the two types of perforations is not significant. Through experiments on plates with similar porosities (about 10%) and staggered perforations with different sizes, Tian et al. (2016) showed that the size and diameter of the perforations do not meaningfully influence the damping coefficient. Also, by performing experiments on two plates with similar porosities (5%) but different perforations, Li et al. (2013) demonstrated that the plates have the same damping coefficient at low KC numbers. These studies indicate that at low KC numbers, the governing parameter is the perforation ratio and not the size of the perforations. Hence, recommended, in numerical simulations in which modeling perforations is difficult, and equivalent plate with a single perforation can be used.

Another component which can potentially influence the damping coefficient is the array of perforations. By carrying out the experiments on vertical plates with similar porosities, Bayazit (2014) showed that the square-array hole pattern causes a higher pressure drop than the staggered-array hole pattern. Therefore, the arrangement of the perforations is another important parameter which needs to be investigated further in horizontal perforation plates.

5.2. The effects of free surface on the damping coefficient of plates

Another important parameter influencing the hydrodynamic behavior of plates is the boundary conditions of the free surface. The reason for this is that when heave plates are sufficiently close to the free surface, it is possible for their damping coefficient to be influenced by the radiation waves induced by the oscillations of the model. In this situation, the vortex shedding caused by the oscillations of the plates can cause scatter with creating waves in the free surface (Garrido-Mendoza et al., 2014). At free surface, this damping includes both viscous damping and radiation damping. Some studies have been carried out on the effectiveness of the draft of these plates. Lindholm et al. (1965) showed that the presence of a free surface can have a significant influence on the properties of oscillating plates(frequencies), provided that its draft is smaller than half of the plate's diameter. However, using experimental results, Prislin et al. (1998) showed that interaction between the oscillating plate and the free surface occurs at a draft smaller than the diameter of the plate.

5.2.1. Effect of distance from the free surface on the damping coefficient of solid plates

As previously mentioned, as the distance to free surface-to-plate diameter ratio decreases, (R_{depth}<=1), small waves start to appear on the free surface in forced vibration tests. By testing isolated rectangular plates with the dimensions of 400 x 400 and under the influence of the free surface (R_{depth}<=1), Li et al. (2013) stipulated that when the value of $KC/2\pi$ is larger than the thickness-to-diameter ratio (t/d), it is expected the t/d ratio not to be influential. To illustrate the importance of this parameter, the results of the tests carried out by Molin et al. (2008), Garrido-Mendoza et al. (2014), Wadhwa et al. (2009 & 2008), Lopez-Pavon and Souto-Iglesias (2015) on plates in free surface condition have been compared in Fig.11 (left side). According to this figure, for a similar (t/d) ratio and a different R_{depth} ratio, the damping coefficients reported by Garrido-Mendoza et al. (2014) (dark brown) are larger than those reported by Lopez-Pavon and Souto-Iglesias (2015) (green). But, at the same depth ratio (R_{depth}= 0.77), Lopez-Pavon and Souto-Iglesias (2015) (green) and Garrido-Mendoza et al. (2014) (dark blue) reported similar values. This comparison shows that in the similar oscillation frequencies and the R_{depth}<=1, the R_{depth} ratio is a more important than the other parameters.

Also, Fig. 11 (left side) show that as the R_{depth} ratio decreases, the damping coefficient experiences a considerable increase. In fact, it can be mentioned that change in the parameter R_{depth} can completely influence the slope of the curve describing the damping coefficient and shift. Therefore, in this type of condition, the effect of the thickness ratio is very small. This is the cause which in some experimental and numerical studies carried out (i.e. Li et al. (2013)), the effect of thickness on the drag coefficients was not taken into account and only a constant thickness was

assumed. However, although it appears that under normal conditions this assumption holds true, conditions are entirely different in cases in which resonant frequencies occur.

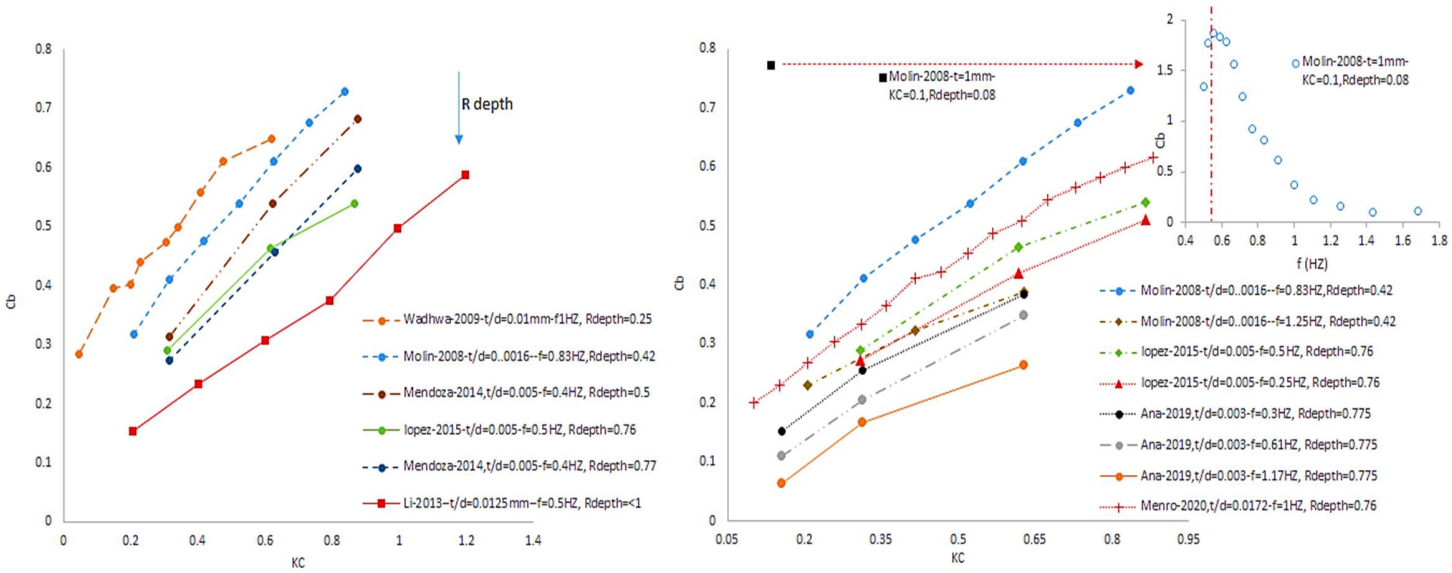

Fig. 11. Comparison of experimental results of solid plates close to free surface

5.2.2. Effect of frequency on the damping coefficient of solid plates

Oscillation frequency is among the important factors of plates when they are under the influence of free surface conditions (Lindholm et al., 1965). Wadhwa et al. (2009) performed experiments on isolated circular steel plates with diameter and thickness of, respectively, 200 mm and a 2 mm. The experiments were carried out close to the free surface and inside a rectangular glass tank (Table 3). Unlike tests carried out far away from the free surface, these tests highlighted the effect of oscillation frequency on the damping coefficient. The results of different studies investigating the effects of free surface on solid plates have been shown in Fig. 11 (right side).

Molin et al. (2008) studied isolated solid plates in the vicinity of the free surface. The authors used circular plates with the diameter and thickness of, respectively, 600 mm and 1 mm, at distances of 5 cm and 25 cm from the free surface (Fig. 11, right side). In that study, it was shown that for the same distance ratio from the surface (R_{depth}= 0.42), the damping coefficient is higher at the frequency of 1.25 Hz than it is at 0.83 Hz. Also, this can be clearly seen in the damping coefficient-frequency curve reported by Molin et al. (2008) for a depth of 0.08 (R_{depth}= 0.08) (Fig. 11, right side-top). The authors also showed that when KC=0.1, the damping coefficient takes on its highest value at the frequency of 0.55 Hz. This clearly demonstrates the important influence of frequency on the hydrodynamic behavior of heave plates under free surface conditions.

Also, as seen in Figure 11 (right side), the experiments of Lopez-Pavon and Souto-Iglesias (2015) and Bezunartea-Barrio et al. (2019) on plates attached to cylinders showed that different oscillation frequencies change the damping coefficient, even at constant distances from the free surface (R_{depth}= 0.76 and R_{depth}= 0.775) and similar thickness-to-diameter ratios (t/d). This can also be observed in the results of Lopez-Pavon and Souto-Iglesias (2015). In that research, the damping

coefficient increases when the frequency is increased from 0.25 Hz to 0.5 Hz. There is, however, a small discrepancy between the results reported by Lopez-Pavon and Souto-Iglesias (2015) and Bezunartea-Barrio et al. (2019). Although in both of those studies the distance from the surface is the same, the difference between the results is due to using different frequencies (0.25 Hz and 0.3 Hz) and different thicknesses. An important point to note in the results of Bezunartea-Barrio et al. (2019) in Fig. 11 (right side) is that the maximum damping value occurs at the frequency of 0.3 Hz. As this frequency increases, the damping coefficient decreases. Generally, these results showed that under free surface conditions, frequency is the governing factor in the behavior of plates subjected to forced oscillation test.

It is also important to point out that closer the oscillation frequencies are to the resonant frequency the damping coefficient increases and vice versa. The resonant frequency in the studies of Lopez-Pavon and Souto-Iglesias (2015) and Bezunartea-Barrio et al., (2019), which have used plates in conjunction with cylinders, are 0.63 Hz and 0.3 Hz, respectively. Therefore, in the study carried out by Ana-Barrio et al., (2019), the frequency of 1.17 Hz caused a significant reduction in the damping coefficient. An example of this can be seen in the damping coefficient-frequency curve reported in the Molin et al. (2008) for R_{depth}= 0.08 (Fig. 11, right side-top). However, and also Molin et al. (2008) have only used isolated plates (Fig. 11-right side). Hence, it is very difficult to determine the resonant frequency. Furthermore, it has to be mentioned that to compare the results of experiments on isolated plates (e.g., Molin et al. (2008)) with other tests involving cylinders attached to plates (e.g., Bezunartea-Barrio et al. (2019); Thiagarajan and Moreno (2020); Molin et al. (2008)), the effects of the cylinder have to be taken into account. Therefore, for a more accurate analysis of plates and also to consider the effect of the cylinder, in the studies by Bezunartea-Barrio et al. (2019), Lopez-Pavon and Souto-Iglesias (2015) and Thiagarajan and Moreno (2020), the added mass was reduced by 10%.

Another parameter that can potentially influence plates close to the free surface is the t/d (thickness/diameter) ratio. In general, under free surface conditions, and considering the damping equation – i.e., Cb=KC*Cd/(4π) – the influence of geometric parameters is far less important. Therefore, the t/d ratio of the plate is far less important, even at low KC numbers (this also diminishes the importance of the amplitude of oscillations).

5.2.3. The effect of perforation on the damping coefficient

Through forced oscillation experiments, Dowine et al., 2000-A & B and Geoffroy (2002) found that perforation plates have a higher level of damping than solid plates at KC numbers smaller than one. Under free surface conditions, Molin et al. (2008) and An and Faltinsen (2013) carried out forced oscillation tests on, respectively, isolated circular and rectangular plates with different porosities and frequencies (0.5, 0.8 Hz). The results of experiments on perforation plates showed that perforation is a more influential factor (Fig. 12). The results of Molin et al. (2008) obtained for low KC numbers and similar frequencies and distance from the free surface (Fig. 12) showed that the damping coefficient of these plates increase when the perforation ratio reaches to about 10%. Then, as the perforation ratio increases to 20%, the damping coefficient decreases compared to solid plates.

This can also be seen in the results reported by An and Faltinsen (2013) (Fig. 12, left side), in which when the perforation increases from 7.9% to 15.89%, the damping coefficient experiences a decrease. Therefore, these results demonstrate that at low frequencies and under free surface conditions, choosing an optimized value for the perforation results in an increase in the damping coefficient.

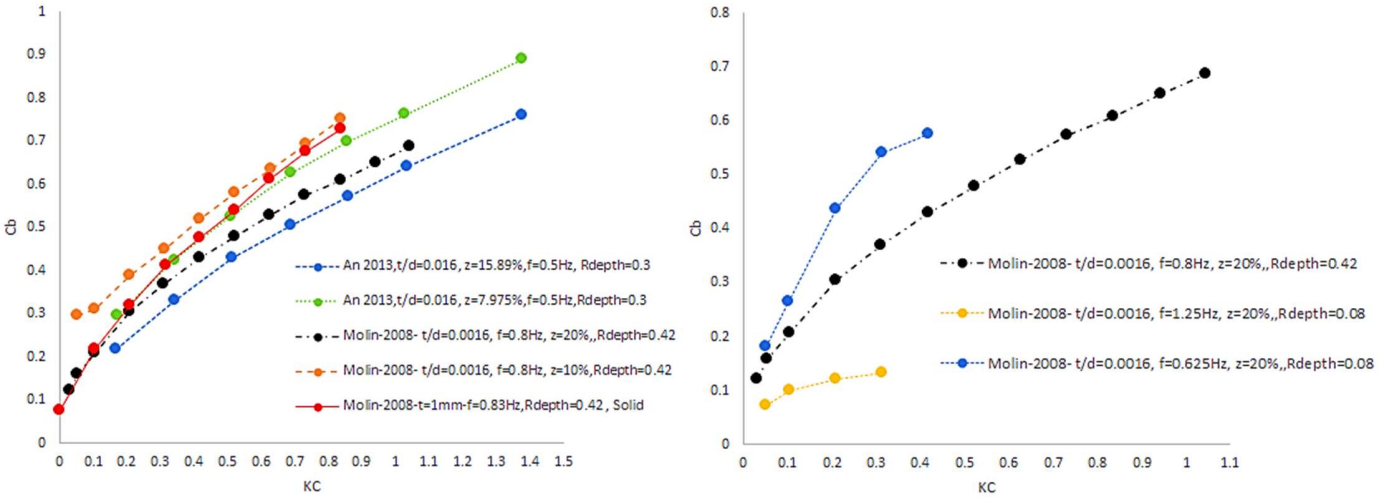

Figure 12: comparison of the experimental results obtained from perforation plates under free surface conditions

5.2.4. Effect of frequency on the damping coefficient of perforated plates

In forced oscillation tests under free surface conditions, as it is the case for solid plates, the influence of oscillation frequency on perforation plates is also significant. The results of An and Faltinsen (2013) have been shown in Fig. 13 in the form of a Cb-frequency diagram for a KC number of 0.69 (KC= 0.69) for indicating the influence of frequency on the drag coefficient.

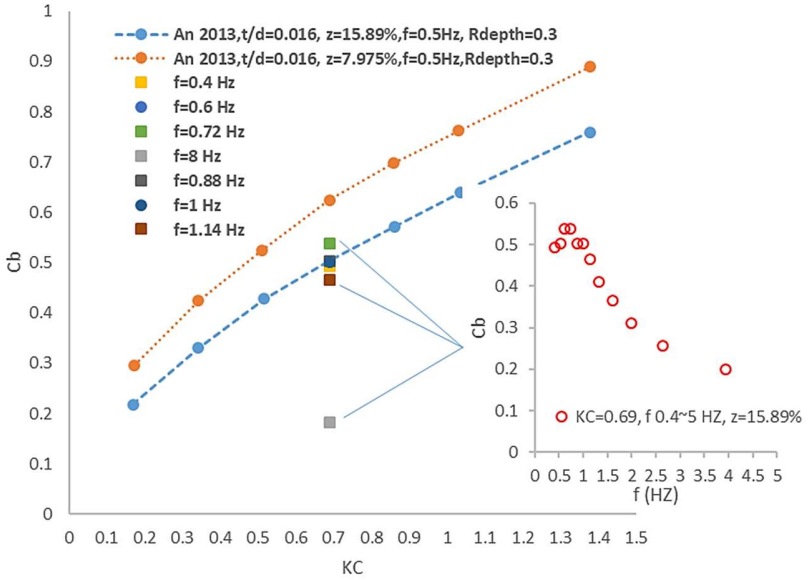

Fig. 13. Comparison of experimental results of perforation plates close to free surface

The results show that at KC=0.69, the highest damping coefficient occurs at a frequency of 0.72 Hz.

Also, as the frequency increases from 0.4 Hz to 0.72 Hz, the damping coefficient undergoes an increase, until it starts to decline upon reaching a frequency of 1.14 Hz. Comparing the results with different frequencies (Fig. 13, Cb-KC diagram) shows that, in general, as the R_{depth} ratio becomes a smaller, the influence of frequency becomes more pronounced. Generally, at oscillation frequencies higher than 1 Hz, small values of distance from R_{depth} ratio lead to a considerable decrease in the damping coefficient. This has also been observed for solid plates.

6. Effects of the scaling

In experimental models, some uncertainties can skew the results. One of these uncertainties is the scale of the models. Today, the results of experiments on scaled models (the Froude method) are considered to be reliable. However, when it comes to general constants such as viscosity, there are uncertainties which stem from the scaling of the Reynolds and Froude numbers (Windt et al., 2018). This uncertainty is far more important at low KC numbers than it is at high KC numbers. The reason is that at low KC numbers, the effects of the scale for the model can lead to the results being overestimated (Mundon et al., 2017). Also, the infinitely small forces at KC numbers tending toward zero need to be measured. To investigate the effects of scale, the results of experimental models with different scales (1:20~80) – which were based on the initial model of the turbine of the Hiprwind 1.7MW project – were compared

The properties of the scaled models are given in Table 4. In all of these studies, the draft of the plate is smaller than its diameter ($R_{depth}<1$). The results of all of the models, therefore, are under the influence of free surface. In Fig. 14, the changes in damping coefficient with respect to the KC number are compared for different scales based on the R_{depth} ratio of the plate. In Fig. 14, although the models with different scales and the same R_{depth} ratio behave in a somewhat similar manner, some differences can be seen. These might be due to:

- Difference in the frequency of oscillations: This parameter is important, particularly when the plate is under free surface conditions. Therefore, selecting a suitable frequency of oscillations can be instrumental in reaching more realistic results and diminishing the scale-associated uncertainty in forced oscillation tests. The resonant frequencies of models with the scales 1:20, 1:27, and 1:45 are 0.63 Hz, 0.4 Hz, and 0.3 Hz, respectively. Therefore, it is expected for the frequency of smaller models (1:80, Menro) to be below 0.3 Hz.
- Amplitude of oscillations: In forced oscillation tests, using a scaled model and an appropriate KC number can reduce the effects of these uncertainties (Bezunartea-Barrio et al., 2019). This also is compatible with the dimensionless damping coefficient equation.

Since these tests (Table 4) are mostly focused on $R_{depth}<1$ and KC<1, the influence of frequency of oscillations are rather important. However, the effects of the plates thickness still needs to be acknowledged when the uncertainties of scaled models in unbounded fluid are being discussed. Other parameters that need to be discussed in terms of the uncertainties associated with scaled models are the solidity, perforation and perforation size (in perforated plates).

Table 4 :Main dimensions of the platform (prototype and model scale, 1:20).

CHARACTERISTIC	SYMBOL	PROTOTYPE	SCALE 1:80, THIAGARAJAN AN MENRO, 2020;	SCALE 1:45, BEZUNARTEA-BARRIO ET. AL,(2019)	SCALE 1:27, BEZUNARTEA-BARRIO ET. AL,(2019)	SCALE 1:20, LOPEZ-PAVON AND SOUTO-IGLESIAS, 2015	SCALE1:20, GARRIDO-MENDOZA ET AL., 2014
HEAVE PLATE DRAFT	h (m)	15.5	0.19	0.341	0.562	0.77	0.5, 0.77
COLUMNS DIAMETER	Dc (m)	7	0.088	0.156	0.257	0.35	0.354
HEAVE PLATE DIAMETER	D (m)	20	0.25	0.44	0.725	1	1
HEAVE PLATE THICKNESS	td (mm)	*	4.3	1.3	2.2	5	5
HEAVE PLATE DEPTH-DIAMETER RATIO	R_{depth}(h/D)	0.775	0.76	0.775	0.775	0.775	0.5, 0.77
HEAVE PLATE THICKNESS-DIAMETER RATIO	td/D	*	0.0172	0.003	0.003	0.0049	0.005
LEG MASS	M (Kg)	663000	-	7.1	31.5	82.83	-

***** FULL SCALE HEAVE PLATE STEEL THICKNESS NOT AVAILABLE
- LEG MASS NOT AVAILABL

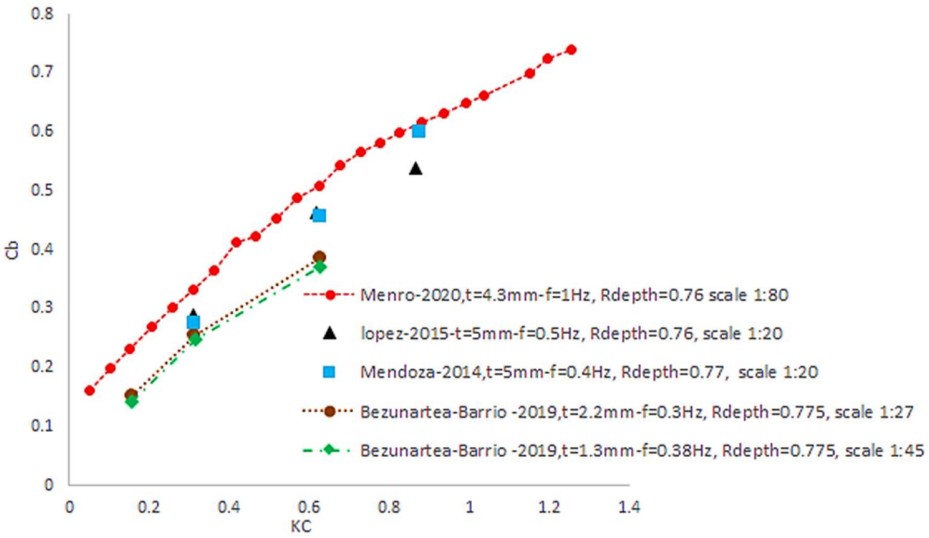

Fig. 14. Comparison of experimental results of plates with different scales

7. Conclusion

The strategies and ways in which heave plates are utilized are important in the effective control and movement management of floating structures against ocean waves. This study presents a deep investigation of the behavior of heave plates and introduces reliable solutions to compare the results of different researchers regarding the hydrodynamic performance of plates.

In this study, in addition to the other parameters, a new parameter – i.e., plate edges area-to-plate area ratio (Re/a) – has been used as basis to compare the results in the unbounded fluid flow (R_{depth}>1). The parameter Re/a provides a better comparison of the results of different studies

investigating models with varying geometric properties. By decreasing the ratio to just above 0.1 (Re/a>0.1), we witness an increase in the damping coefficient. Further decreasing the value of the ratio to below 0.1 (Re/a<0.1) leads to a decrease in the damping coefficients for almost all cases. Therefore, it is recommended the area of the heave plate to be approximately 10 times the area of the edges to maximize the damping mechanism of heave plate.

The evaluation carried out in the unbounded fluid flow showed that the pressure drop at the outer edges is higher than it is at the inner edges (hole). The reason is that at the outer edges, there is an evident discrepancy between the velocities of the fluid particles the edge and the outer area surrounding the edges. Thus, as the array of the inner edges is closer to the outer edges, more damping is created. Also, these studies indicate that as the KC number increases (until KC>0.1), the effect of perforation increasing the drag coefficient becomes considerably weak, and further increase in the perforation of the plate causes the drag coefficient to fall below that of solid plates. This is due to the disturbance in the flow of fluid in the wake of the plate by perforations, which prevents the creation of a vortex. The optimal perforation ratio is about 10% to 15%.

Investigation of the experimental data of different researchers in the unbounded fluid flow showed that the frequency of oscillations does not exert profound influence on the damping coefficient. It does, however, cause some scatter in the damping coefficient-KC number curve. As flow visualization showed, at low KC numbers, it is unlikely to see the collision of the vortices shed from the two edges, instead the collision of the secondary vortices in each cycle (the separation length is almost constant) often taking place. Secondly, assessing the equation of the non-dimensional damping coefficient (Equation 6) reveals that there is no direct correlation between the damping coefficient and frequency of oscillations. However, it can be demonstrated that the frequency may influence the damping coefficient as a weak effect by solving the integral part of the drag coefficient equation (Equation 4).

When heave plates oscillating near free surface, change in the value of R_{depth} can significantly shift the slope of the damping coefficient diagram. Under such circumstances (oscillating near free surface), the effects of the frequency of oscillations are rather important.

At the end, in addition to suitable thickness, spaces from the free surface and perforation, locating in the transition area, it is clearly evident that when the interaction of heave plate with surrounding flow developing from the interface regime into a unidirectional regime, it can often result in maximizing the damping coefficient in different ocean conditions.

8. References

Abazari, A., Behzad M., Thiagarajan K.P., 2020. Hydrodynamic performance of multiple co-axial heave plates with different diameters. Ships Offshore Struct. 15(4), 380–392.

Abazari, A., Behzad M., Thiagarajan K.P., 2019. Hydrodynamic performance of multiple co-axial heave plates with different diameters, Ships and Offshore Structures, DOI: 10.1080/17445302.2019.1625109.

An, S., Faltinsen, O.M., 2013. An experimental and numerical study of heave added mass and damping of horizontally submerged and perforated rectangular plates. J. Fluids Struct. 39, 87–101.

Bayazit, Y., Sparrow, E. M., & Joseph, D. D., 2014. Perforated plates for fluid management: Plate geometry effects and flow regimes. International Journal of Thermal Sciences, 85, 104–111. doi:10.1016/j.ijthermalsci.2014.0.

Börner, Th., Alam, M.R., 2015. Real time hybrid modeling for ocean wave energy converters. Renewable and Sustainable Energy Reviews. 43, 784–795.

Buchanan, H., 1968. Drag on flat plates oscillating in incompressible fluids at low reynolds numbers. NASA-TM-X-53759, N69-17466.
Brown, P.W., 1964. The Effect of Configuration on the drag of oscillating damping plates. Davidson Laboratory, Stevens Institute of Technology. Report. 1021.
Bearman, P. W., Downie, M. J., Graham, J. M. R., & Obasaju, E. D., 1985. Forces on cylinders in viscous oscillatory flow at low Keulegan-Carpenter numbers. Journal of Fluid Mechanics, 154(-1), 337. doi:10.1017/s0022112085001562.
Brown, A., Thomson, J., & Rusch, C., 2018. Hydrodynamic Coefficients of Heave Plates, With Application to Wave Energy Conversion. IEEE Journal of Oceanic Engineering, 1–14. doi: 10.1109/JOE.2017.2762258
Bezunartea-Barrio, A., Fernandez-Ruano, S., Maron-Loureiro, A., Molinelli-Fernandez, E., Moreno-Buron, F., Oria-Escudero, J., Rios-Tubio, J., Soriano-Gomez, C., Valea-Peces, A., Lopez-Pavon, C., and Souto-Iglesias, A., 2020. Scale effects on heave plates for semi-submersible floating offshore wind turbines: case study with a solid plain Plate. ASME. J. Offshore Mech. Arct. Eng. 142(3), 031105.
Benjamin W. Floan & Ephraim M. Sparrow., 2012. Fluid flow in heat exchangers whose flow passages contain periodically deployed tubes, Numerical heat transfer, part A: Applications: An International Journal of Computation and Methodology, 62:2, 81-94. http://dx.doi.org/10.1080/10407790.2012.685125.
Castro, I., 1971. Wake characteristics of two-dimensional perforated plates normal to an air-stream. Journal of Fluid Mechanics, 46(3), 599-609. doi:10.1017/S0022112071000727.
Cavaleri, L., Mollo-Christensen, E., 1981. Wave response of a spar buoy with and without a damping plate. Ocean Eng. 8, 17–24.
Chakrabarti, S., Barnett, J., Kanchi, H., Mehta, A., Yim, J., 2007. Design analysis of a truss pontoon semi-submersible concept in deep water. Ocean Eng. 34, 621–629.
Chua, K.H., Clelland, D., Shuang, S., Sworn, A., 2005. Model experiments of hydrodynamic forces on heave plates. In: 24th International Conference on Offshore Mechanics and Arctic Engineering, OMAE.
Cong, L.f., Teng, B., 2019. Hydrodynamic characteristics of square heaving plates with opening under forced oscillation. China Ocean Eng. 33, 637–648.
Coe, R. G., Rosenberg, B. J., Quon, E. W., Chartrand, C. C., Yu, Y.-H., van Rij, J., & Mundon, T. R., 2019. CFD design-load analysis of a two-body wave energy converter. Journal of Ocean Engineering and Marine Energy. doi:10.1007/s40722-019-00129-8.
Chwang, A. T., & Chan, A. T., 1998. Interaction between porous media and wave motion. Annual Review of Fluid Mechanics, 30(1), 53–84. doi:10.1146/annurev.fluid.30.1.53.
Chwang, A. T., 1983. A porous-wavemaker theory. Journal of Fluid Mechanics, 132(-1), 395. doi:10.1017/s0022112083001676.
J. F. Dalzell, 1978. Non-linear forces on oscillating plates: review and analysis of the literature. Stevens Institute of Technology, Davidson Laboratory, Hoboken, NJ, Report SIT-DL-78-9-2031
Darcy, H.,1856. Les Fontaines Publiques de la Ville de Dijon, Dalmont, Paris.
Downie, M., Graham, J. M., Hall, C., Incecik, A., & Nygaard, I., 2000-A. An experimental investigation of motion control devices for truss spars. Marine Structures, 13(2), 75–90. doi:10.1016/s0951-8339(00)00010-1.
Dowine, M.J., Wang, j., & Graham,J.M.R., 2000-B. The effectiveness of porous damping divces. Proccedings of the tenth International offshore and polar engineering conference, II, 418-425. Seattle, USA.
De bernardinis, B., Graham J.M.R., Parker K.H., 1981.Oscillatory flow around disks and through orifices. J Fluid Mech. 102, 279, 99.
Evans, D.V., Peter, M.A., 2011. Asymptotic reflection of linear water waves by submerged horizontal porous plates. J. Eng. Math. 69 (2-3), 135–154.
Forchheimer, P.H., 1901. Wasserbewegung durch boden, Zeitz. Ver. Duetch Ing, Vol. 45, pp. 1782-1788.
Fischer, F.J., & Gopalkrishnan, R., 1998. Some Observations on the Heave Behavior of Spar Platforms. *Journal of Offshore Mechanics and Arctic Engineering-transactions of The Asme, 120*, 221-225.
Faltinsen, O.M., 1993. Sea Loads on Ships and Offshore Structures, Cambridge Ocean Technology Series, Cambridge University Press.
Griffin, O.M., & Ramberg, S.E., 1976. Vortex shedding from a cylinder vibrating in line with an incident uniform flow. Journal of Fluid Mechanics, 75, 257-271. doi.org/10.1017/S0022112076000207.
Garrido-Mendoza, C.A., Thiagarajan, K., Bouscasse, B., Colagrossi, A., Souto-Iglesias, A., 2014. Numerical investigation of the flow features around heave plates oscillating close to a free surface or seabed. In: ASME 33rd International Conference on Ocean, Offshore and Arctic Engineering (OMAE).

Graham, J. M. R., 1976. Turbulent flow past a porous plate. Journal of Fluid Mechanics, 73(03), 565. doi:10.1017/s002211207600150x.
Graham, J. M. R., 1980. The forces on sharp-edged cylinders in oscillatory flow at low keulegan-carpenter numbers, Journal of Fluid Mechanics. 97(1), 331-346.
Glanville, R.S., Paulling, J.R., Halkyard, J.E. and Lehtinen, T.J., 1991. Analysis of the spar floating drilling production and storage structure, Proceedings of the 23rd Offshore Technology Conference, OTC, Houston, Texas.
Halkyard, J., 1996. Status of Spar Platforms for Deepwater Production Systems. In: Proceedings of 6th Int Offshore and Polar Eng Conf, Los Angeles.
Geoffroy, G., 2002. Added mass and damping of solid or porous disks in heave, Thesis, University of Western Australia; Perth..
Henry, C.J., 1967. Linear damping characteristics of oscillating rectangular flat plates and their effect on a cylindrical float in waves. Davidson Laboratory, Stevens Institute of Technology. Report. 1183, AD-657636.
He, H., Troesch , A. W., Perlin, M.,2007. Hydrodynamics of damping plates at small KC numbers. Proceedings of the IUTAM Symposium on Fluid-Structure Inter- action in Ocean Engineering, Hamburg, Germany, pp.93–104. doi:10.1007/978-1-4020-8630-4-9.
Ishihara, T., Zhang, S., 2019. Prediction of dynamic response of semi-submersible floating offshore wind turbine using augmented Morison's equation with frequency dependent hydrodynamic coefficients. Renew. Energy 131, 1186–1207.
Jonkman, J. M., 2007, Dynamics Modeling and Loads Analysis of an Offshore Floating Wind Turbine, NREL, Technical Report No. NREL/TP-500- 41958.
J. Li, S. Liu, M. Zhao, B. Teng, 2013. Experimental investigation of the hydrodynamic characteristics of heave plates using forced oscillation. Ocean Eng. 66, 82–91.
Keulegan GH, Carpenter L.H., 1958. Forces on Cylinders and Plates in an Oscillating Fluid. Journal of Research and National Beaureu of Standards.
Karimirad, M., & Moan, T. (2011). Extreme Dynamic Structural Response Analysis of Catenary Moored Spar Wind Turbine in Harsh Environmental Conditions. Journal of Offshore Mechanics and Arctic Engineering, 133(4), 041103. doi:10.1115/1.4003393.
Kim, M.H., Ran, R., Zheng, W., Bhat, S. and Beynet, P., 1999. Hull/Mooring Coupled Dynamic Analysis of a Truss Spar in Time-Domain. In: Proceedings of the 9th ISOPE Conference, Brest, France.
Kaufer D., Cosack N., Boker C., Seidel M., Kuhn M., 2009. Integrated analysis of the dynamics of offshore wind turbines with arbitrary support structures. In: Proceedings of the European Wind Energy Conference EWEC, Marseille, France.
Lindholm U.S., Kana D.D., Chu W.H., Abramson H.N., 1965. Elastic vibration characteristics of cantilever plates in water. Journal of Ship Research.
Lake, M., He, H., Troesch, A.W., Perlin, M., Thiagarajan, K.P., 2000. Hydrodynamic coefficient estimation for TLP and spar structures. J. Offshore Mech. Arct. Eng. 122, 118–124.
Lopez-Pavon, C., Souto-Iglesias, A., 2015. Hydrodynamic coefficients and pressure loads on heave plates for semis-submersible floating offshore wind turbines: a comparative analysis using large scale models. Renew. Energy 81, 864–881.
Lefebvre, S., Collu, M., 2012. Preliminary design of a floating support structure for a 5MW offshore wind turbine. Ocean Engineering. 40, 15–26.
Malavasi, S., Messa, G., Fratino, U., & Pagano, A., 2012. On the pressure losses through perforated plates. Flow Measurement and Instrumentation, 28, 57–66. doi:10.1016/j.flowmeasinst.2012.0
Malavasi, S., Messa, G. V., Fratino, U., & Pagano, A., 2015. On cavitation occurrence in perforated plates. Flow Measurement and Instrumentation, 41, 129–139. doi:10.1016/j.flowmeasinst.2014.1
Mentzoni, F., Kristiansen, T., 2019. A semi-analytical method for calculating the hydrodynamic force on perforated plates in oscillating flow. In: Proceedings of the International Conference on Offshore Mechanics and Arctic Engineering, OMAE.
Mentzoni, F., Kristiansen, T., 2020. Two-dimensional experimental and numerical investigations of perforated plates in oscillating flow, orbital flow and incident waves. Applied Ocean Research. 97, 102078.
Mentzoni, F., Kristiansen, T., 2019. Numerical modeling of perforated plates in oscillating flow. Applied Ocean Research. 84, 1–11.
Magee, A.R., Sablok, A., Maher, J., Halkyard, J., Finn, L. and Datta, I., 2000. Heave plate effectiveness in the performance of truss spars, Proceedings of the International Conference on Offshore Mechanics and Arctic Engineering, New Orleans, pp. 469–479.
McIver M., 1985. Diffraction of water waves by a moored, horizontal, flat plate. J. Eng. Math. 8, 279–301.

MARTIN, P. A., FARINA, L., 1997. Radiation of water waves by a heaving submerged horizontal disc. Journal of Fluid Mechanics. 337, 365–379.
Molin, B., 2001. On the added mass and damping of periodic Arrays of fully or partially porous disks. Journal of Fluid and Structures. 15(2), 275-290.
Molin, B., Nielsen, F.G., 2004. Heave added mass and damping of a perforated disk below the free surface, in: Proceedings of the 19th International Workshop on Water Waves and Floating Bodies, Cortona, Italy.
Molin B., Remy F., Rippol, T., 2008. Experimental study of the heave added mass and damping of solid and perforated disks close to the free surface. In: Maritime industry, ocean engineering and coastal resources. Taylor & Francis, 879–87.
Molin, B., 2011. Hydrodynamic modeling of perforated structures. Applied Ocean Research, 33(1), 1–11. doi:10.1016/j.apor.2010.11.003.
MAULL, D. J., MILLINER, M. G., 1978. Sinusoidal flow past a circular cylinder. Coastal. Eng. 2,149.
Mahesh J.R., Nallayarasu, S., Bhattacharyya, S.K., 2021. CFD approach to heave damping of spar with heave plates with experimental validation. Applied Ocean Research. 108, 102517.
McNown, J.S., Keulegan, G.H., 1959. Vortex Formation and Resistance in Periodic Motions. In: Proceedings of ASCE, Engineering Mechanics Division.
McKnown, J.S., Learned, A.P., 1978. Drag and inertia Forces on a Cylinder in Periodic Flow. Journal of the Waterway, Port, Coastal arid Ocean Division of ASCE. 104(2) 1 978, 2147-250.
Mundon, T.R., Rosenberg, B.J., van Rij, J., 2017. Reaction body hydrodynamics for a multi-DOF point-absorbing WEC. In: Proceedings of the 12th European Wave and Tidal Energy Conference, Cork, pp. 997–1–10.
Martin, D., Li, X., Chen, C.-A., Thiagarajan, K., Ngo, K., Parker, R., Zuo, L., 2019. Numerical Analysis and Wave Tank Validation on the Optimal Design of a Two-Body Wave Energy Converter. Renewable Energy.
Nallayarasu S., Sreeraj R., Murali M., 2014. Effect of hull geometry on the hydrodynamic response of spar in regular waves. J Ships Offshore Struct. 9(1), 22–37.
Online in website: http://image.guardian.co.uk/sys-images/Guardian/pictures/2012/3/15/1331836785722/Taschen-book-oilrig-008.jpg.
Online in website: http://www.gabreport.com/2012/08/wind-turbines-ride-the-wave- to-renewable-energy-future., Cermelli, C.A.,2014. Wind turbines ride the wave to renewable energy future.
Online in web site: https://www.nationalgeographic.com/animals/article/140220-five-striking-wave-and-tidal-energy-concepts., Brian Hanwerk, February 21, 2014.
Penalba, M., Davidson, J., Windt, C., Ringwood, J. V., 2018. A high-fidelity wave-to-wire simulation platform for wave energy converters: Coupled numerical wave tank and power take-off models. Applied Energy. 226, 655–669.
Prislin, I., Blevins, R.D., Halkyard, J.E., 1998. Viscous damping and added mass of solid square plates. In: Proceedings of the 17th International Conference on Offshore Mechanics and Arctic Engineering, OMAE98, Lisbon, Portugal, Paper 0316, 7 pp.
Prislin, I., Halkyard, J., DeBord, F., Collins, J. I., & Lewis, J. M., 1999. Full-Scale Measurements of the Oryx Neptune Production Spar Platform Performance. Offshore Technology Conference. doi:10.4043/10952-ms.
Rusch, C.J., Mundon, T.R., Maurer, B.D., & Polagye, B.L., 2020. Hydrodynamics of an asymmetric heave plate for a point absorber wave energy converter. *Ocean Engineering, 215*, 107915.
Roddier, D., Cermelli, C., Weinstein, A., 2009. Wind Float: A Floating Foundation for Offshore Wind Turbines—Part I: Design Basis and Qualification Process. Ocean Eng. Part. 4, 845–853.
Rajagopalan K, Nihous G., 2016. Study of the force coefficients on plates using an opensource numerical wave tank. Ocean Eng.118, 187–203.
Stephens, D. G., Scavullo, M. A., United States., & Langley Research Center.,1965. Investigation of air damping of circular and rectangular plates, a cylinder, and a sphere. Washington, D.C: National Aeronautics and Space Administration.
Singh, S., 1979. Forces on bodies in oscillatory flow. Ph.D. thesis University of London.
Sandvik, P.C., Solaas, F., Nielsen F.G., 2006. Hydrodynamic forces on ventilated structures. In: Proceedings of the Sixteenth International Offshore and Oolar Engineering Conference, ISOPE.
Sireta, F. X., Thiagarajan, K., Molin, B., & Pistani, F. (2008). Hydrodynamic coefficients of porous plates and application to subsea deployment. In Y. S. Choo, & D. N. Edelson (Eds.), *Proceedings of the Marine Operations Specialty Symposium 2008* (Singapore ed., Vol. 1, pp. 1-5). National University of Singapore.
Shen, W.jun., Tang, Y.G., Liu, L.Q., 2012. Research on the hydrodynamic characteristics of heave plate structure with different form edges of a spar platform. China Ocean Eng. 26, 177–184.

Sarpkaya T., Isaacson M., 1981. Mechanics of wave forces on offshore structures. Van Nostrand Reinhold Company, New York.
Sarpkaya, T.,1975. Forces on Cylinders and Spheres in a Sinusoidally Oscillating Fluid. Journal of Applied Mechanics, 42(1), 32. doi:10.1115/1.3423549.
Sudhakar, S., Nallayarasu, S., 2011. Influence of heave plate on hydrodynamic response of Spar hull. 30th Ocean Offshore and Arctic Engineering Conference (OMAE), Rotterdam, the Netherlands.
Tao, L., Dray, D., 2008. Hydrodynamic performance of solid and porous heave plates. Ocean Engineering. 35(10), 1006 – 1014.
Subbulakshmi, A., & Sundaravadivelu, R., 2016. Heave damping of spar platform for offshore wind turbine with heave plate. Ocean Engineering, 121, 24–36. doi:10.1016/j.oceaneng.2016.05.00.
Singh, S. 1979 Forces on bodies in oscillatory flow. Ph.D. thesis, University of London.
Tao, L., Molin, B., Scolan, Y.M., Thiagarajan, K., 2007. Spacing effects on hydrodynamics of heave plates on offshore structures. J. Fluids Struct. 23, 1119–1136.
Tao, L., Cai, S., 2004. Heave motion suppression of a Spar with a heave plate. Ocean Eng. 31(5), 669–692.
Tao, L., Cai, S., 2004. Heave motion suppression of a Spar with a heave plate. Ocean Engineering. 31(5-6), 669–692.
Tao L., Thiagarajan K., 2003(b). Low KC flow regimes of oscillating sharp edges. II. Hydrodynamic forces. Appl Ocean Res. 25(2), 53–62.
Tao, L., Thiagarajan, K., 2003 (a). Low KC flow regimes of oscillating sharp edges, I: vortex shedding observation. Applied Ocean Research. 25 (1), 21–35.
Tao, L., Cheng, L., Thiagarajan, K., 1999. Numerical estimation of hydrodynamic heave damping of a vertical cylinder with appendages. Proc. 9th Int. Offshore Polar Eng. Conf 7, 490–495.
Taylor, G., 1956. Fluid Flow in Regions Bounded by Porous Surfaces. Proceedings of the Royal Society A: Mathematical, Physical and Engineering Sciences, 234(1199), 456–475. doi:10.1098/rspa.1956.0050
Li, Y., Teng, B., 2002. Wave action on maritime structures. 2nd Edition, Oceanic 20 Express, Beijing, China
Takaki, Mikio, and Sang-Min Lee., 2003. Hydrodynamic Forces on Submerged-Plate Heaving Near a Free Surface. In Proceedings of The Thirteenth International Offshore and Polar Engineering Conference, Honolulu, Hawaii, USA.
Thiagarajan, K.P., Troesch, A.W., 1994. Hydrodynamic heave damping estimation and scaling for tension leg platforms. J. Offshore Mech. Arct. Eng. 116, 70.
Thiagarajan, K., Troesch, A.W., 1998. Effects of appendages and small currents on the hydrodynamic heave damping of TLP columns. J Offshore Mech Arctic Eng. 120(1), 37–42.
Thiagarajan, K., Moreno, J., 2020. Wave Induced Effects on the Hydrodynamic Coefficients of an Oscillating Heave Plate in Offshore Wind Turbines. Journal of Marine Science and Engineering. 8(8), 622.
Thiagarajan, KP, Datta, I, Ran, AZ, Tao, L, & Halkyard, JE., 2002. Influence of Heave Plate Geometry on the Heave Response of Classic Spars. Proceedings of the ASME 2002 21st International Conference on Offshore Mechanics and Arctic Engineering. 21st International Conference on Offshore Mechanics and Arctic Engineering, Volume 1. Oslo, Norway. June 23–28, 2002. pp. 621-627. ASME. https://doi.org/10.1115/OMAE2002-28350
Tian, X., Tao, L., Li, X., Yang, J., (2016). Hydrodynamic coefficients of oscillating flat 0.15⩽KC⩽3.15. Journal of Marine Science and Technology. 22(1), 101–113.
Tian, X., Yang, J., Li, X., Peng, T., 2013. Experimental Investigations on the Hydrodynamic Characteristics of Heave Plate. In: ASME 2013 32nd international conference on ocean, offshore and arctic engineering.
Tanner, P., Gorman, J. and Sparrow, E. (2019), "Flow–pressure drop characteristics of perforated plates", International Journal of Numerical Methods for Heat & Fluid Flow, Vol. 29 No. 11, pp. 4310-4333. https://doi.org/10.1108/HFF-01-2019-0065
Vu, K.H., Chenu, B., Thiagarajan, K.P., 2004. Hydrodynamic damping due to porous plates. In: Proceedings of the World Scientific and Engineering Academy and Society, WSEAS, Corfu, Greece, 5 pp (available at ⟨ http://www.wseas.us/e-library/conferences/corfu2004/papers/488-360.pdf ⟩, 01/18/2022).
Yu, Y.-H., Tom, N., & Jenne, D., 2018. Numerical Analysis on Hydraulic Power Take-Off for Wave Energy Converter and Power Smoothing Methods. Volume 10: Ocean Renewable Energy. doi:10.1115/omae2018-78176.
Yang, J., Tian, X., Li, X., 2014. Hydrodynamic characteristics of an oscillating circular disk under steady in-plane current conditions. Ocean Engineering, 75, 53–63.
Yang, J., Tian, X., Li, X., 2014. Hydrodynamic characteristics of an oscillating circular disk under steady in-plane current conditions. Ocean. Eng. 75, 53–63.
Wang, J., Berg, S., Luo, Y.H., Sabloc, A., Finn, L., 2001. Structural Design of the Truss Spar – An Overview. Proc. Of 11th ISOPE Conference, Stavanger, Norway.
Wang, J., Downis, M.J., Graham, J.M.R., 2002. Mean and Oscillatory flows past porous plates. Proceedings of ASME International Mechanical Engineering Congress and Exposition; New Orleans, Louisianam.

Woolam, E.W., 1978. Drag Coefficients for Flat Square Plates Oscillating Normal tb Their Planes in Air. NASA CR-66544, March 1968, AIAA Paper 78-1692, Sept.
Wadhwa, H., & Thiagarajan, K., 2008. PIV Study of Vortex Shedding Flow Pattern induced by Circular Disks in Heave Motion. In P. O'Neill, & K. Thiagarajan (Eds.), *Proceedings of the 5th Australian Conference on Laser Diagnostics in Fluid Mechanics and Combustion* (Perth, Western Australia ed., Vol. 1, pp. 35-38). The University of Western Australia.
Wadhwa, H., & Thiagarajan, K. P., 2009. Experimental Assessment of Hydrodynamic Coefficients of Disks Oscillating Near a Free Surface. Volume 4: Ocean Engineering; Ocean Renewable Energy; Ocean Space Utilization, Parts A and B. doi:10.1115/omae2009-79671
Windt, C., Davidson, J., & Ringwood, J. V., 2018. High-fidelity numerical modelling of ocean wave energy systems: A review of computational fluid dynamics-based numerical wave tanks. Renewable and Sustainable Energy Reviews. 93, 610–630.
Wood, C. J., 1964. The effect of base bleed on a periodic wake. The Aeronautical Journal, 68(643), 477-482.
Zdravkovich, M. M., 1981. Review and classification of various aerodynamic and hydrodynamic means for suppressing vortex shedding. Journal of Wind Engineering and Industrial Aerodynamics, 7(2), 145–189. doi:10.1016/0167-6105(81)90036-2.
Wu, J.H., Wan, Z.P., Fang, Y., 1998. Wave reflection by a vertical wall with a horizontal submerged porous plate. Ocean Eng. 25 (9), 767–779.
Zhang, S., Ishihara, T., 2018. Numerical study of hydrodynamic coefficients of multiple heave plates by large eddy simulations with volume of fluid method. Ocean Eng. 163, 583–598.
Zhang, C., Huang, H., & Lu, X.-Y., 2020. Effect of trailing-edge shape on the self-propulsive performance of heaving flexible plates. Journal of Fluid Mechanics, 887. doi:10.1017/jfm.2019.1076
Zhu, L., Lim H.C., 2017. Hydrodynamic characteristics of a separated heave plate mounted at a vertical circular cylinder. Ocean Eng.131, 213–223.
Zhou, B. Z., Ning, D. Z., Teng, B., & Bai, W., 2013. Numerical investigation of wave radiation by a vertical cylinder using a fully nonlinear HOBEM. Ocean Engineering, 70, 1–13. doi:10.1016/j.oceaneng.2013.04.01